REMOTE
STORAGE

THESIS
1
2000

MICHIGAN STATE UNIVERSITY LIBRARIES
3 1293 02074 1041

LIBRARY
Michigan State
University

This is to certify that the

thesis entitled

REMOTE SENSING OF LEAF TISSUE NITROGEN CONTENT
AND DISEASE SEVERITY IN CREEPING BENTGRASS
AND ANNUAL BLUEGRASS USING NEAR INFRARED SPECTROSCOPY

presented by

GEOFFREY JORDAN RINEHART

has been accepted towards fulfillment
of the requirements for

M.S. degree in Crop and Soil Sciences

Major professor

Date 3/22/00

O-7639 *MSU is an Affirmative Action/Equal Opportunity Institution*

REMOTE STORAGE RSF

PLACE IN RETURN BOX to remove this checkout from your record.
TO AVOID FINES return on or before date due.

DATE DUE	DATE DUE	DATE DUE
MAY 07 2013		

2/17 20# Blue FORMS/DateDueForms_2017.indd - pg.5

REMOTE SENSING OF LEAF TISSUE NITROGEN CONTENT AND DISEASE SEVERITY IN CREEPING BENTGRASS AND ANNUAL BLUEGRASS USING NEAR INFRARED SPECTROSCOPY

By

GEOFFREY JORDAN RINEHART

A THESIS

Submitted to
Michigan State University
in partial fulfillment of the requirements
for the degree of

MASTER OF SCIENCE

Department of Crop and Soil Sciences

2000

ABSTRACT

REMOTE SENSING OF LEAF TISSUE NITROGEN CONTENT AND DISEASE SEVERITY IN CREEPING BENTGRASS AND ANNUAL BLUEGRASS USING NEAR INFRARED SPECTROSCOPY

By

Geoffrey Jordan Rinehart

Site-specific application of nutrients and pesticides based upon the specific needs of turfgrass plants has the potential to save money and reduce the potential threat of polluting the environment. The objectives of this study were to develop a method to determine N content of leaf tissue and disease status of brown patch (*Rhizoctonia solani* Kuehn) and dollar spot (*Sclerotinia homeocarpa* Bennett) on creeping bentgrass (*Agrostis stolonifera* Huds.) and annual bluegrass (*Poa annua* var. *reptans* Hausskn) using a direct light visible/near (VIS-NIR) infrared scanning monochromator. Nitrogen was applied at rates of 0, 1.2, 2.4, 3.6, and 4.8 g N/m^2 periodically over two growing seasons to creeping bentgrass and annual bluegrass mowed at heights of 5 mm and 14 mm. Absorbance was expressed as "log 1/reflectance" between 400 and 2500 nm once color differences were evident. After spectrometer readings were attained, clippings were harvested from each plot and analyzed for N using a dry combustion analyzer. Modified partial least squares regression analysis using the wavelengths from the entire spectrum demonstrated a relationship between leaf tissue N content and canopy reflectance (r^2= 0.78-0.92). Wavelengths which illustrated the best association between lab values for the raw spectrum occurred at wavelengths 670, 1450, and 1930 nm and correspond to chlorophyll

a transmission, a primary overtone O-H stretch attributable to water, and an O-H stretch attributable to water, lignin, protein, nitrogen, and starch, respectively.

Brown patch and dollar spot are two common diseases of cool season turfgrass in the United States. As governmental and public scrutiny of golf course maintenance practices increases, superintendents are beckoned to balance playability with fewer fungicide inputs. Categorical disease symptom severity ratings of brown patch and dollar spot were made on different turfgrass swards and associated spectra obtained. Discriminant analysis of the data yielded categorical accuracy. In the dollar spot study, 20 out of 193 samples (10.3%) were classified incorrectly using categories associating spectra with diseased areas, areas close to the disease that appeared healthy, and healthy areas away from the disease symptoms. In the brown patch study there were only 29 misses out of a total of 336 samples (8.6%) using three classification categories consisting of severe and medium disease and healthy areas. These results suggest the feasibility of developing a VIS-NIR sensor for the detection of disease severity. Future research should address how various stresses interact to affect the spectral reflectance of the turfgrass plant. These results indicate the potential for developing a real-time remote sensor for site specific nutrient and fungicide applications in turfgrass management.

ACKNOWLEDGEMENTS

Without the assistance of many people along the way, this product would not have been possible. For the guidance I received during this project, I express appreciation to my major professor, Dr. James Baird, and committee members, Dr. Joseph Vargas and Dr. Gene Safir. I would like to express thanks to Ron Calhoun, Dr. Baird's technician; Nancy Dykema and Ron Detweiler for their assistance during the disease project; Frank Roggenbuck for help during the greenhouse experiments, and Joe Kroening at the Toro Company for assistance in the nitrogen analyses. For help concerning the statistical analysis and interpretation much gratitude goes to Dr. John Shenk and Dr. Mark Westerhaus at Infrasoft International; Dr. Syed Dara at the Toro Company; Dr. Oliver Schabbenberger, formerly at Michigan State; and Dr. Carl Ramm, Department of Forestry.

Special thanks are certainly in order to all of my fellow graduate students in the Departments of Crop and Soil Sciences, Botany and Plant Pathology, and Horticulture. I would like to especially recognize graduate students in the turfgrass group and those in Dr. Baird's lab, Beau McSparin, Ryan Goss, and Susan Redwine. A word of appreciation goes our undergraduate workers, Stephanie Dysinger and Dan Lamb.

Finally, and by no means least, I would like to thank my family: my father, Douglas; my mother, Vivian; my sister, Christen; and my brother, Stuart.

TABLE OF CONTENTS

LIST OF TABLES

LIST OF FIGURES

LIST OF ABBREVIATIONS

AOTF	Accoustical optical tunable filter
C: N	Carbon to nitrogen ratio
FAD	Flavine adenine dinucleotide
GIS	Geographic information systems
GPS	Global positioning system
GOGAT	Glutamate synthase
IR	Infrared
K	Potassium
LAI	Leaf area index
MSR	Modified stepwise regression
MPLSR	Modified partial least squares regression
N	Nitrogen
NAD	Nicotinamide adenine dinucleotide
MIR	Mid infrared
MoCo	Molybdenum cofactor
NDVI	Normalized Difference Vegetation Index
NiR	Nitrite reductase
NIR	Near-infrared
NIRS	Near-infrared spectroscopy
NIST	National Institute of Standards and Testing
NR	Nitrate reductase
NUE	Nitrogen use efficiency
P	Phosphorous
PAR	Photosynthetically active radiation
PCA	Principal component analysis
PLS	Partial least squares
PTM	Precision Turf Management
PNSI	Plant Nitrogen Spectral Index
PSNT	Pre-sidedress nitrogen test
R	Reflectance
r^2	Coefficient of determination
RCBD	Random complete block design
RMS	Root mean square
SD	Standard deviation
SECV	Standard error of cross validation
SEC	Standard error of calibration
SED	Standard error of the difference
SEP	Standard error of performance
SSM	Site Specific Management
TCA	Tricarboxylic acid
UAN	Urea ammonium nitrate
USGA	United States Golf Association
VRT	Variable rate technology

CHAPTER ONE

INTRODUCTION

Pesticides and fertilizers are an integral part of golf course management today as golfers expect a high level of course maintenance and playability. Accompanying this phenomenon is the increased potential for these inputs to have detrimental environmental impact if applied without educated decisions about the needs of the turfgrass ecosystem. As golfers' expectations increase, golf course superintendents are forced to balance course playability with environmental considerations. Increasing public and governmental scrutiny will continue to put a premium on a superintendent's ability to use necessary inputs judiciously. In light of this, it is important that fertilizer and pesticide resources be used responsibly to both reduce environmental impact and maintain a reasonable turfgrass quality.

Site specific management (SSM) or Precision Turf Management (PTM) refers to the practice of assessing a property's variability and adjusting management practices accordingly. Site variability can be affected by a number of factors including soil texture and fertility, terrain, slope and aspect, mowing height, drought stress, disease pressure, turfgrass species and cultivar composition, and by environmental factors such as light quality and intensity and air flow characteristics.

The four primary components of SSM involve the global positioning system (GPS), geographic information systems (GIS), sensing, and variable rate technology (VRT). The GPS refers to a collection of 24 orbiting satellites which are oriented circumspherically about the earth and were originally established for military navigation purposes. A GPS receiver communicates via radio signal with appropriate satellites and

the distance from the satellites to the reciever is calculated. Using trigonometric principles, the reciver's exact location can be determined and described in coordinates of latitude and longitude. The precision of the transmitter measurements varies according to sophistication and cost. Current technology allows precision down to millimeter increments. Sub-meter resolution would be required for practical application on golf courses, which require greater precision than production agriculture.

Geographic information systems (GIS) refers to any of a number of computer software programs which integrate information about site variability into a visual format, typically in the form of a map. It provides a method by which spatial information may be captured, stored, analyzed, displayed, retrieved and overlaid (Krzanowski et al., 1992). Geographic information systems allow a manager to overlay maps containing information about various parameters of interest and graphically observe relationships that may exist among the parameters.

A cost-effective process for acquiring spatial information is currently the most limiting aspect of SSM in the realm of turfgrass science. Real-time sensing is a component of precision management which is necessary in order to collect a large volume of data efficiently, quickly, and relatively inexpensively and is essential to developing the full potential SSM. A sensor based upon reflectance from the canopy could provide a cost- and labor-effective strategy for assessing turf leaf N content and disease symptoms.

The information can be geographically referenced with GPS and assimilated with GIS. Based upon the sensor data, a spray vehicle equipped with a manifold of variable-output nozzles can vary the application rate of an input such as a fertilizer or pesticide.

The efficient use of chemical inputs on golf courses will help decrease environmental impact. Variable rate technology (VRT) is the process of adjusting the rate of applied inputs according to the assessed needs of the plant. Information acquired in real-time can be processed so that appropriate spray applications are conducted and referenced using GPS and GIS. The goal of sensor-based VRT is "to instantaneously adjust application rates based on sensor measurements of fertility [or other factors] as an applicator travels across the field." (Stone et al., 1993). Effective use of this technology will sponsor precise applications of inputs needed to retain turfgrass quality and reduce the total amount of inputs needed.

The sensing aspect of SSM is the focus of this research and involves scanning turf with a spectrometer which is able to detect reflectance of the turf canopy in the range of 400 to 2500 nm. The objectives of this research were to: 1) determine if an association exists between leaf N content and reflectance from the canopy; 2) determine how the relationship is affected by turfgrass species or cultivar, mowing height; and soil type; 3) to establish a spectral signature characterizing the presence of *Rhizoctonia solani* and *Sclerotinia homeocarpa* on turf.

LITERATURE REVIEW

NITROGEN USES IN THE TURFGRASS PLANT

Nitrogen (N), potassium(K) and phosphorous(P) are referred to as macronutrients because they are the mineral nutrients required in the greatest amounts for proper plant nutrition, excluding atmospheric elements carbon, oxygen, and hydrogen which are intrinsic to many plant biochemical functions (Marshner, 1995). Nitrogen is required by the plant for the production of amino and nucleic acids, enzymes, and proteins and the proper functioning of chlorophyll (Epstein, 1972). Although 78% of the atmosphere is composed of N, atmospheric N is not available to turfgrass because of the diatomic molecule's high triple bond energy. Nitrogen is present in many forms, but nitrate (NO_3^-) and ammonium (NH_4^+) are the major sources utilized for plant uptake. These forms of N are produced by aerobic microorganisms decomposing organic matter or by the input of synthetic fertilizers. Symptoms of N deficiencies include shoot stunting, decreased tillering, and development of chlorosis symptoms in older tissue because N is phloem-mobile (Marshner, 1995). Turfgrass typically contains 3-5% N by dry weight. Turfgrass N requirements depend on soil nutrient holding capacity, natural precipitation or irrigation, mowing height, traffic, and species or cultivar (Beard, 1982). Unlike other nutrients, there is no reliable test for soil N. Although rules of thumb are recognized as guidelines, ultimate N application decisions are subjective and based upon a manager's experience with a particular turf (Turgeon, 1991; Beard, 1982). Sufficient N should be supplied to maintain density, adequate recuperation and shoot growth and color (Beard, 1982). Excessive N can contribute to excessive thatch, greater disease incidence, a restricted root system, lower recuperative capacity due to energy being allocated to aerial

growth, and environmental stress tolerance on account of depleted carbohydrates (Beard, 1982; Couch, 1995).

NITROGEN CYCLING IN THE PLANT COMMUNITY

There are several fates of N applied to turf. Nitrogen can be taken up by the plant, stored in the thatch/soil, volatilized, denitrified or leached. Starr and Deroo (1981) reported that 19-27% of applied N may be immobilized in thatch. Relatively high N levels within thatch can sustain high microbial populations. Leaching (loss of NO_3^--N through the soil profile) is most prevalent with fast-release fertilizers and sandy soils. Volatilization refers to gaseous phase losses of N as ammonia; these losses increase with higher temperatures and relative humidity. Denitrification involves the reduction of nitrate and nitrite to nitric oxides and N_2. The process occurs mainly in waterlogged or anaerobic soil conditions as microbes use nitrate as an electron acceptor instead of oxygen.

Mineralization and immobilization are the two dominant processes involving N in soil organic matter turnover and are strongly affected by the carbon:nitrogen (C:N) ratio of organic material present in a plant's rootzone. Mineralization occurs as aerobic heterotrophic organisms conduct aminization and ammonification, converting organically-bound N to NH_4^+. Ammonification is the process where fungi, bacteria, and actinomycetes transform amino acids from organic matter into ammonia. Mineralization generally increases with increasing temperature and adequate moisture. Conversely, immobilization refers to the conversion of inorganic N to organic N and one of the main factors contributing to this is the C:N ratio of the organic matter present. In a high C:N organic matter environment, microbes will use ammonium and nitrate from the soil and

effectively immobilize it from use by plants. Subsequently, immobilized N can be mineralized with the addition of high N organic matter (Tisdale et al., 1993).

NITROGEN ASSIMILATION BY THE PLANT

Ammonium assimilation begins with NH_4^+ uptake into roots and ends with its incorporation into amino acids, amides, proteins and other nitrogen complexes. Upon plant uptake, either protons are released for charge compensation or anion uptake increases, depending on the soil ionic environment. Accordingly, roots are the primary site of assimilation since they can better dispose of excess protons than shoots. Uptake is optimal in neutral pH soils and decreases with an increase in acidity. Ammonium can be dissociated to ammonia (NH_3) or directly assimilated into amino acids and amides in the root and subsequently amino acids in the shoot using carbon skeletons from the tricarboxylic acid (TCA) cycle (Marshner, 1995).

The nitrate assimilation pathway is cornerstone to incorporating inorganic N into organic compounds. Contrasting ammonium uptake, high nitrate levels correspond with an increase in uptake of organic cations by the roots. Nitrate reduction can occur in roots and shoots. In low concentrations, a greater percentage of nitrate is reduced in the roots and with greater concentrations, more is translocated for reduction in the shoots. Maximum nitrate assimilation occurs when leaf expansion rate is high (Salisbury and Ross, 1992; Marshner, 1995).

As opposed to ammonium, nitrate must be reduced to NH_4^+ in order to be incorporated into organic structures. Nitrate assimilation occurs via a specific transport

system and involves a two-step reaction which is spatially separated:

$$NO_3^- \rightarrow NO_2^- \quad \text{[Eq. 1]}$$
$$NO_2^- + 6e^- + 8H^+ \rightarrow NH_3 \quad \text{[Eq. 2]}$$
$$NO_3^- + 8H^+ + 8e^- \rightarrow NH_3 + 2H_2O + OH^- \quad \text{[Eq. 3]}$$

The first reaction [Eq. 1] is catalyzed by *Nitrosomonas* bacteria and the second step [Eq. 2] is catalyzed by *Nitrobacter* bacteria. The electron donor in the processes is the compound NAD(P)H. Good correlation has been observed between light intensity and nitrate reduction, but it is unclear whether this is due to the increased light itself or confounded by the fact that there are a greater number of carbon skeletons into which additional fixed N could be assimilated (Marshner, 1995).

Nitrate reductase (NR), located in the cell cytoplasm, is a dimer molecule composed of a heme group, FAD, and a molybdenum cofactor (MoCo) and is located in the cytoplasm. Nitrate reductase is regulated by enzyme synthesis and breakdown, reversible inactivation, and the concentration of the substrate present (Solomonson and Barber, 1990). Nitrite reductase (NiR) is located in chloroplasts and proplastids of roots and other non-green tissue (Fig. 1.1). Nitrite rarely accumulates as this step of the reaction is extremely rapid. Ferrodoxin is the primary electron donor in the reaction.

Ammonia can be toxic in high concentrations, but is usually rapidly incorporated into organic compounds. Almost all ammonia produced by ammonium oxidation, nitrate reduction, and photorespiration is processed by the glutamate-glutamine synthesis pathway. With the addition of NH_3, glutamate synthetase catalyzes the production of glutamine from glutamate. Light stimuli provide the impetus for 2-oxogluterate and glutamate to be exported from the stroma to the cytoplasm, thus aiding nitrate reduction and ammonium assimilation (Woo et al., 1987).

Glutamine synthetase and glutamate synthase (GOGAT) are the two primary enzymes involved in ammonia assimilation. Glutamate synthase, facilitated by ferrodoxin or NADPH, catalyzes the transfer of $-NH_2$ from glutamine to 2-oxoglutarate. This results in the production of two glutamate molecules, one of which can be used for maintenance in the cycle and one that can be used for biosynthesis of low molecular weight nitrogen compounds. When high amounts of ammonia are present, both glutamate molecules can accept ammonia molecules (Fig. 1.2).

Glutamate and glutamine are used for the synthesis of amides, ureides, amino acids, peptides and high molecular weight compounds such as proteins. Glutamate can be used for amino acid synthesis by transamination reactions which are catalyzed by aminotransferases located in the cytosol, chloroplasts, and other organelles. Carbon skeletons used for amino acid synthesis are obtained from photosynthesis, the tricarboxylic acid (TCA) cycle, and glycolysis reactions. Proteins are polypeptides constructed from amino acids and coupled by peptide bonds in a condensation reaction in cellular ribosomes. Glutamine and asparagine are the primary low molecular weight compounds produced by the pathway. Amino acids, amines, peptides, and ureides are also produced and are used for transient storage and long distance transport from roots to shoots.

Images in this thesis are presented in color.

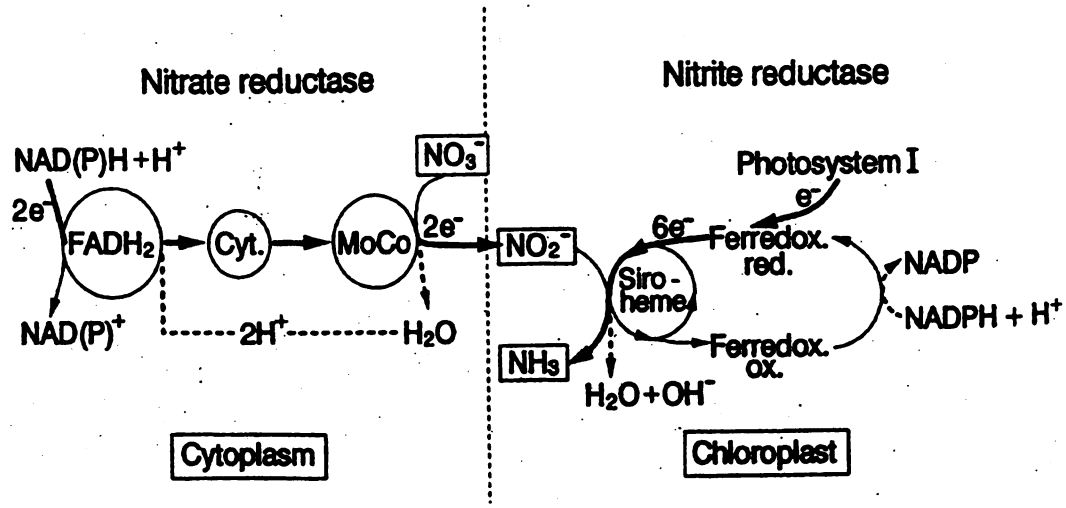

Figure 1.1. Schematic representation of the sequence of nitrate assimilation in leaf cells. (Adapted from Marshner, 1995).

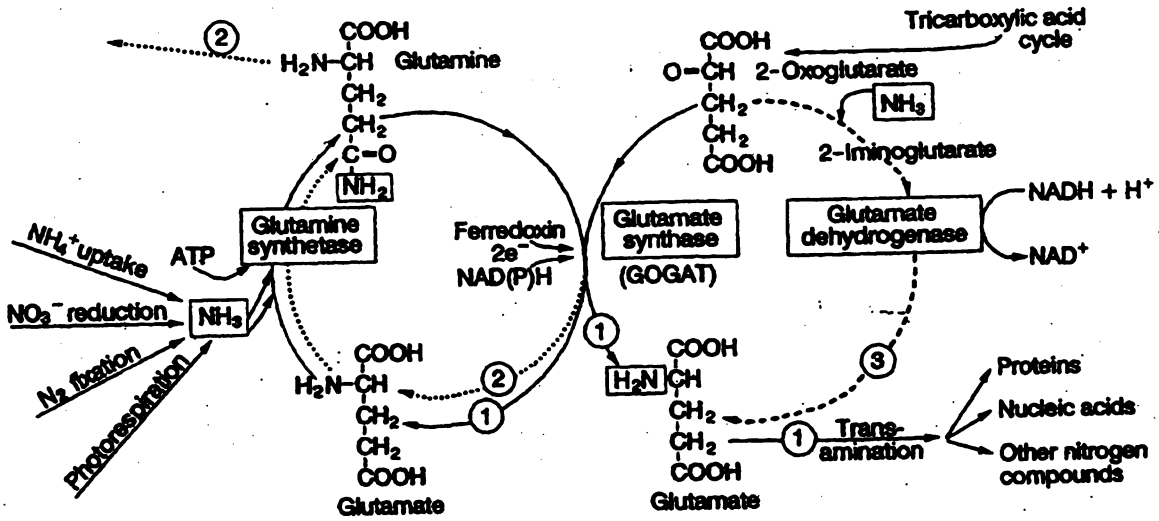

Figure 1.2. Model of ammonia assimilation pathways (1,2) Glutamine-synthetase-glutamate synthase pathway, with low NH_3 supply (1) and with high NH_3 supply (2). (3) Glutamate dehydrogenase pathway. (Adapted from Marshner, 1995).

BROWN PATCH (*Rhizoctonia solani* Kuehn)

Brown patch disease is caused by the fungus *Rhizoctonia solani*. Other species (*R. oryzae, R. cerealis*) are known to be pathogenic to turfgrass as well (Burpee and Martin, 1992). Brown patch disease occurs on many commonly cultivated turfgrass species. The fungus produces tan to brown mycelium that are 4-15 μm in diameter with constricted dolipore septae and no clamp connections (Couch, 1995). In the absence of optimal growth conditions, the organism survives by dark brown sclerotia produced in the plant tissue, or as a saprophyte, among the soil and thatch. As the fungus begins to actively grow at temperatures of 15-20 C, the sclerotia provide a nutrient source as the mycelia resume growth (Vargas, 1994). Hyphal aggregation leads to the formation of appressoria and these infection cushions penetrate the leaf between epidermal cells or through stomates (Shurtleff, 1953). Ultimately, injury can be inflicted upon the plants in two ways, infection of the plant by mechanical pressure and tissue necrosis caused by enzymatic degradation of the cell walls (Couch, 1995).

Brown patch disease symptoms vary with grass type, mowing height, and environmental conditions. Individual leaf blade symptoms are characterized by tan to brown leaf lesions, which can grow to envelop the entire leaf blade turning it light brown and necrotic; lesions sometimes develop reddish-brown margins. Stems, crowns and roots can be infected by the pathogen. Typical symptoms on a given turf sward include foliar necrosis in brown to straw-colored irregular brown patches. A dark purple smoke ring can develop on the leading front of the disease symptoms, especially on low-cut turf <13 mm, and can be seen most frequently in the presence of early morning dew. Disease development of the disease is favored by nighttime temperatures >16 C and > 10 h of leaf

wetness (Burpee and Martin, 1992). Mycelia begin active growth at 15-20 C and initial infections can occur at 21-26 C (Vargas, 1994). Temperatures between 27- 29 C are optimal for infection by epidermal cell penetration and colonization is most rapid at 29-32 C accompanied by high humidity. Above 32 C mycelia development is slowed. High humidity and prolonged periods of leaf wetness, as well as high N levels relative to normal levels of P and K can encourage symptom development. Since dew and plant guttation water contain high levels of nutrients favored by the fungus, removing dew by poling or early morning irrigation is recommended (Vargas, 1994). Chemical control is attained with preventative applications of flutolanil, chlorothalonil, iprodione, or azoxystrobulin applied at 14-28 day intervals when favorable environmental conditions persist.

DOLLAR SPOT (*Sclerotinia homoeocarpa* Bennett)

Dollar spot is one of the most prevalent diseases on golf courses in North America, Australia and Japan (Smiley, 1983). Symptoms appear as circular and sometimes sunken bleached straw-colored to brown patches approximately 2-5 cm in diameter (Vargas, 1994). As the disease severity increases, spots can coalesce, blighting large areas of turf. Individual leaves have bleached, water-soaked tan lesions with a reddish-brown margin often appearing as an hourglass pattern. Mycelia appear as grayish white to white and cottony and are especially visible in the presence of morning dew. Under low N conditions, dollar spot symptoms are more prevalent, assuming adequate P and K levels (Couch and Bloom, 1960).

The fungus rarely produces apothecia, and if present, they do not contain viable reproductive organs such as ascospores or conidia (Smiley, 1983). It is believed that the

pathogen is primarily dispersed via equipment and traffic and survives as dormant mycelia on leaf foliage. Active growth resumes as favorable conditions develop. The pathogen affects the plant by producing a toxin in the foliage, which upon translocation prevents root elongation, causes browning of the roots and encourages root thickening and a decrease in root hairs. Toxin production is optimal between 15.5-26.8 C (Endo, 1964).

Cultural management strategies that reduce the duration of leaf wetness such as poling greens, watering after dark and in the early morning to wash off dew and guttation water from leaves can alter environmental conditions that are optimal for the disease. Chemical control is attained with applications of triadimefon, propiconazole, cyproconazole, thiophanate-methyl, benomyl, iprodione, fenarimol, or chlorothalonil when environmental conditions favorable to disease development persist (Couch, 1995).

PROPERTIES OF LIGHT

The electromagnetic spectrum contains radiant energy described by parameters of "wavelength", "frequency", and energy (Fig. 1.3). The entire spectrum covers 20 orders of magnitude from cosmic rays which contain the most energy to radio waves containing the least. In the middle of the spectrum are ultraviolet (200-400 nm range), visible (400-700 nm), and near infrared (700-2500 nm range) wavelengths (Kemp, 1991). The visible portion of the spectrum is known as "photosynthetically active radiation" since this is the portion utilized by plants for photosynthesis.

Light is a unique form of energy in that it exhibits properties of both waves and particles. A light wave is a "transverse electromagnetic wave" in the shape of a sine where electric and magnetic fields are present perpendicularly to the direction of wave

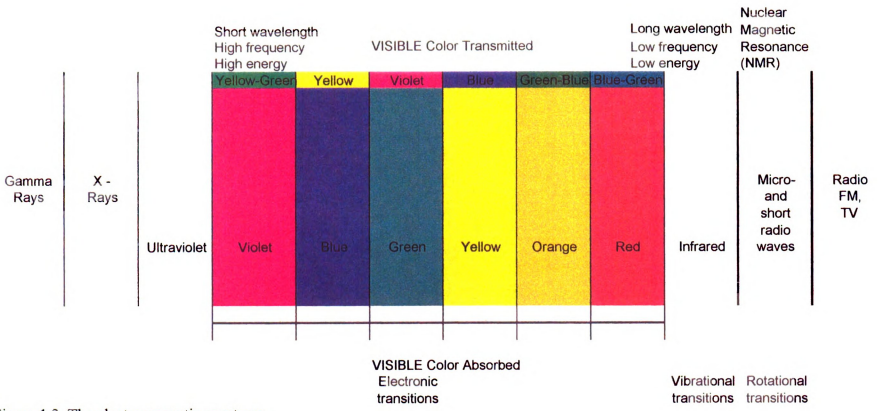

Figure 1.3. The electromagnetic spectrum.

propagation (Taiz and Zeiger, 1991). Wave properties are characterized by the wavelength, the distance between two crests of the sine curve (nm); frequency, how many crests occur in a given distance (Hz, /s); and the pattern. The equation $c = \lambda\nu$ represents the speed of light, 2.998×10^8 m/s, where λ is the wavelength and ν is the frequency; thus, λ and ν are inversely proportional. Particle (photon) properties of light consist of discrete packets of energy called "quanta." Energy is explained by the equation $E = h\nu$ where E is energy in joules, h is Planck's constant (6.626×10^{-34} J•s), and ν is the frequency of the radiation (/s or Hz). Subsequently, $E = hc/\lambda$ so a radiation wavelength is inversely proportional to the energy which it contains.

Once light strikes an object it may be reflected, transmitted, or absorbed (Woolley, 1971). Reflected light is returned to the atmosphere at a different angle from which it struck the object incidentally. Transmitted light energy passes through the object without being absorbed; transmittance is negligible through turfgrass because of its dense canopy (Trenholm et al., 1999). Energy absorption occurs when incident light energy matches the exact amount of energy needed to move electrons from a ground to excited state. Excitation may be due to translational, vibrational, or rotational changes which occur in the organic molecule. Since electron orbits represent discrete energy levels, electrons require exact amounts of energy for excitement from one to another. The relationship between transmission of energy through the sample and the concentration of the absorbing molecular bonds is described by Beer's Law. Energy light absorbed is proportional to the molecule or pigment concentration of interest and is expressed as log (1/reflectance) (Shenk and Westerhaus, 1993c).

An absorption spectrum illustrates the change in absorption of electromagnetic energy by an object across a range of wavelengths. When transition of a molecule from one energy state to another occurs at a specific wavelength, it corresponds to the energy absorbed at that wavelength. The molecule will only absorb the energy if it is equal to that required for the transition. Due to differences in bond and molecular structure (and the energy required for transition), organic molecules absorb energy differentially. Highly conjugated molecules such as plant pigments chlorophyll, anthocyanins, carotenoids and xanthophylls absorb at higher energy wavelengths in the visible spectrum. Organic molecule functional groups such as hydroxyls, carbonyls, and amines, absorb at lower energy wavelengths in the near infrared spectrum. Humans have the ability to differentiate light in the visible region from 400-700 nm. Contained in this range is what we traditionally think of as a "spectrum of colors." (Fig.1.3). All objects absorb light differentially to varying degrees and the human eye perceives an object as a certain color because that color is reflected the most. Likewise, plant pigments absorb differentially across the spectrum so that a plant's perceived color, or appearance of an object determined by eye response, consists of wavelengths which are absorbed the least. For instance, in examining the absorption spectrum of chlorophyll one finds that it absorbs the greatest amount of light in the red and blue regions (75-90% absorbance) and absorbs the least in the green region so that when chlorophyll, the dominant pigment is present, plant leaves appear green (<20% absorbance). With an instrument that measures "greenness" one could indirectly measure chlorophyll content. Since nitrogen is an important component of and closely correlated to chlorophyll, measures of "greenness" would give an indication of the nitrogen status of the plant (Thomas and Oerther, 1972).

Chlorophyll produces a green color because it absorbs the least in the green region (~550 nm). When chlorophyll absorbs light, the light energy causes the chlorophyll molecules to be excited to a higher state from its initial "ground" state. The excited energy contained within the molecule can undergo one of three fates. The molecule may undergo fluorescence where it re-emits the energy as it falls from its lowest excited state back to its ground state. This release is characterized by a phenomenon called the Stokes Shift as the energy is re-emitted at a wavelength approximately 10 nm longer than that which it was absorbed. Second, the molecule may return to its ground state without re-emitting energy as a photon, but as heat. Finally, the molecule may activate the plant's photosystem network, stimulating the electron transport chain in photosynthesis (Taiz and Zeiger, 1991).

Near Infrared Spectrum

The near infrared (NIR) region of the spectrum ranges from 700-2500 nm. Functional groups such as $=CH_2$ (1090-1167, 1390-1400, 1406-1446, 1616-1626, and 2260-2510 nm), O-H water bonds (984-996, 1010, 1150, 1406-1416, 1788-1796 and 1936-1946 nm), N-H protein bonds (1048-1052, 1508-1516, 2050-2066, 2176-2186, and 2296-2308 nm), and other N-H groups (1464, 1470, 1480-1506, 1518-1536, 1906-1916, 1976-1996, and 2046-2056 nm) and organic molecules absorb energy in the NIR (Winisi, 1999). Absorbance of NIR radiation corresponds to energy required for changes in the internal vibrational frequencies of the molecule and functional groups of organic molecules absorb NIR radiation differentially. A fundamental vibration occurs when the energy supplied is proportional to the energy required to change the dipole moment of the molecule so that the vibrational energy absorbed causes it to change from its ground state to its first excited state (Zabik, 1997). Absorbance by organic functional groups produces

characteristic bands in local areas of the near infrared spectrum (Zabik, 1997). Absorption bands can be characterized by three criteria: location, height, and width. Near infrared absorption patterns are very complex, existing in a mosaic of overtones, combination bands and repititive bands. Typical NIR spectra exhibit a convolution of Lorentzian and Gaussian distributions and may consist of seven to ten peaks with many "shoulders" (Shenk and Westerhaus, 1993c). Band overlapping and composite banding makes it difficult to estimate the three criteria so mathematical functions are needed to provide accurate estimates of band locations. Additional confounding may occur due to particle size multiplicative response, confounding with visible overtones in 1100-1400 region, and confounding with mid-infrared information contained in the 2300-2500 nm region.

Reflected light can undergo a scattering effect as it strikes an object. Scatter is a function of the diffuse nature (roughness) of the surface (Shenk and Westerhaus, 1993c). Particle size can contribute to scatter, which can cause peak distortion and larger particles make peaks appear higher than they should. Conversely, surface reflectance, or the "shininess" of an object can "squash" peaks to appear lower than they should. Essentially, the information contained in a NIR absorbance spectrum provides useful insight into the physical and chemical composition of a substance (Shenk and Westerhaus, 1999). Every substance has a unique spectral composite "signature" contributed to by scatter, surface reflectance and absorption of chemical bonds (Shenk and Westerhaus, 1999) and diffuse reflectance properties correlate to changes in chemical composition (Morra et al., 1991). Ideally, since a spectrometer can detect wavelengths over a wide spectrum of electromagnetic radiation, a specific band could be used to

detect differences attributable to nitrogen status or disease presence in the turf canopy. However, more practically, a combination of wavelengths would be used to develop a model which characterizes the anomaly of interest.

A fundamental absorption may have several overtones, or secondary vibrations which decrease in intensity (amplitude) and energy level, and exist in the range of 700-1800 nm. Combination bands consisting of two or more overtones of these groups exist in the 1800-2500 nm range. These combination bands indicate rotational and vibrational movements such as stretching, bending, wagging, and rocking of the organic molecule. Stretching vibrations occur at higher frequencies (lower wavelengths) than bending vibrations. Molecular bending can occur in the plane of the molecule or out of the plane. Each deformation absorbs energy of different intensity. Energy striking a compound will be absorbed if it equals the energy required for a molecule to jump to a higher state. The NIR region is composed of harmonic overtones of the functional groups which absorb primarily in the mid-infrared (MIR). Major bands in the NIR region include second and third overtones of O-H, C-H, and N-H functional groups. Theoretically, peak height of the vibrations diminishes with each successive overtone. Molecular absorptions occur with greater intensity as fundamental bands in the MIR region of the spectrum because NIR bands are 10-100 times weaker than those found in the MIR. Organic molecule functional groups O-H, C-H, and N-H absorb energy at different wavelengths due to their stretching, bending and deformation vibrations (Shenk and Westerhaus, 1993c). Shifts in the spectrum related to organic molecules can potentially be associated with physiological changes in the plant. Characteristic wavelengths which indicate the presence of these groups include O-H bonds stretches at 1440 and 1900 nm and N-H

stretches in ranges from 1449-1555 nm and 1800-2080 nm. Within the umbrella of N-H stretches are primary amines (1455-1553 nm), secondary amines (1506-1555), N-H proteins (1535- 1614 nm), nitrites (1800-2080 nm), NH_2 groups (1965-2050 nm) and NH_2 amines (1449-1538 nm) (Shenk and Westerhaus, 1993c).

SPECTROSCOPY

As with any spectroscopic method, proper assessment of a sample for evaluation is affected by several factors. Instruments used to detect visible and NIR spectra must be accurate and repeatable. Temperature, relative humidity, and spectrometer light source and intensity play significant roles in instrument performance. The ambient light surrounding the stage of the sample will have an effect on how the light reflected, absorbed, and transmitted by the sample will be detected by an instrument. In a laboratory setting, enclosed spectrophotometers provide for a means of controlling ambient light surrounding a sample.

Near infrared detection devices typically consist of several components. A source of radiance, usually a tungsten light bulb, is needed to provide consistent illumination of the sample. In order to process the quality of light, once detected, the light is transmitted through a slit to limit radiation to a narrow band. A lens is used to focus a narrow band of radiation and the energy is sent through a wavelength dispersion device to split the energy into its component parts before passing through a focusing lens. The energy is transmitted through another focusing lens before passing through an exit slit and ultimately a photodetector. The placement of the detectors determines if the instrument initially makes a transmission or reflectance measurement. Signal from the detector is

amplified before being converted from analog to digital for computer processing and monitor display.

There are four primary wavelength dispersion devices used in NIR analysis. Filters are used for detection of absorption in specific regions of the spectrum, disallowing passage of light outside the range(s) of interest. In contrast, light emitting diodes emit light energy only at specific wavelengths of interest. Accoustical optical tunable filters (AOTF) are used for liquid solution analysis. Wavelength is controlled by the frequency at which a crystal vibrates. A monochromator is a holographic grating which divides light energy into separate wavelengths at a given interval across the range of detection (Shenk and Westerhaus, 1993c).

Light striking an object may be detected by reflectance, transmittance, folded transmittance or direct light methods. Normal NIR reflectance and transmittance measurements involve holding the sample in a ring cup, exposing it to a light source at a path length of 1 cm in a closed compartment and detecting how much is reflected or transmitted, depending on the location of the photodetector. Folded transmittance measurements are ideal for materials in solution and use a narrower path length of 0.1 mm. All three of these measurements are made in chambers opaque to outside light. In the direct light method, source radiation is introduced directly upon the sample. The reflected radiation is then transmitted via fiber optic cable to the monochromator and, subsequently, the photodetector.

General NIR Applications

Near infrared reflectance measurements are used for analysis of a wide range of agricultural and industrial products (Wetzel, 1983). Notable agricultural applications

have involved measurement of protein, moisture, fat, oil, and prediction of organic carbon and total nitrogen (Wetzel, 1983; Dalal and Henry, 1986). Near infrared spectroscopy (NIRS) has also been used to measure moisture content in soybeans and fat and moisture in meat emulsions (Ben-Gera and Norris, 1968). The fact that NIR has been used successfully for constituent analysis of forages (Norris, 1976; Windham, 1991) lends to its potential effective use in turfgrass analysis.

Near infrared spectroscopy is an attractive alternative to traditional laboratory methods that measure crude protein, acid detergent fiber, fats, moisture and other constituents (Wetzel, 1983; Shenk and Westerhaus, 1991). It provides for rapid analysis of plant constituents and requires minimal sample preparation (Couilliard et al., 1997). Near infrared spectroscopy can accurately measure constituents such as water (O-H bonds) and crude protein (N-H bonds) in the microgram per kilogram range (Roberts et al., 1991). Near infrared spectroscopy does not actually measure N, but measures N-H, from which N and protein can be interpolated (Shenk and Westerhaus, 1991a). Fox et al. (1993) compared reflectance measurements in the NIR region with three other rapid tests for predicting N-supplying capability and grain yield in corn and found that NIRS was as statistically accurate as the pre-sidedress nitrogen test (PSNT) to predict the soil N-supplying capacity and corn response to N.

Prediction equations for forage mixtures and monostands have been developed using NIR (Shenk and Westerhaus, 1991a). Principally used for detecting plant constituents in agriculture, NIR has also been used for carbon and nitrogen analysis in particle-size soil fractions (Morra et al., 1991). Near infrared spectroscopy can be useful because it provides a window into biochemical workings of a plant that reflectance in the

visible range may not. For instance, changes in leaf area index (LAI) can result in changes in NIR region reflectance without altering the visible region reflectance characteristics (Colwell, 1974).

Traditional sample preparation for NIR analysis involves oven-drying the samples to remove moisture before grinding them to insure a uniform particle size. Samples are then packed into a cell for spectral analysis on a laboratory benchtop model instrument. However, use of NIR technology for real-time analysis will require development of a field unit capable of conducting direct light measurements. Successful attempts to analyze unprocessed samples have been accomplished for predicting turf soil profiles (Couilliard et al., 1997).

Data Analysis

Analysis of NIR data is difficult due to factors such as particle size or spectral (particularly water) overtones (Shenk and Westerhaus, 1993c). Two corrections have been developed to reduce interference caused by differences in particle size. First, de-trend, a multiplicative scatter correction described by Barnes et al. (1989), shifts the spectra of interest to be more like a designated "target spectrum", usually an average spectrum of the spectra of interest. Second, a standard normal variate correction can be used so that the standard deviation of each spectrum is 1.0.

Several regression methods may be used to create a prediction equation for using NIR patterns to predict laboratory analysis numbers. Multivariate regression methods such as modified stepwise regression (MSR), neural networks, and partial least squares (PLS) have been used (Shenk and Westerhaus, 1993c). Shenk and Westerhaus (1991b) found that a modified partial least squares regression (MPLSR) had better correlation

than MSR in developing constituent calibration equations for diverse forage mixtures. Comparing the MPLSR method to the MSR method, they demonstrated that MPLSR was similar or better than MSR for predicting crude protein, acid detergent fiber, and in vitro dry matter disappearance for two large groups of forage samples.

Algorithms CENTER and SELECT were developed to identify spectra suitable for calibration development by eliminating samples with extreme or similar spectra. These algorithms use the spectral data across a range of wavelengths with absorbance values expressed as Log (1/R) and an associated reference value for the constituent(s) of interest. The CENTER function computes a principal components file by full-spectrum single value decomposition, which contains all information needed to calculate sample scores and define H (Mahalanobis) values. Principal component analysis (PCA) identifies patterns (also known as eigenvectors or loadings) in certain wavelength regions which contain the most variation attributable to different laboratory values. Principal component analysis also reduces the spectral information into a smaller number of independent factors. The amount of a pattern present in a spectrum is referred to as a score (Shenk and Westerhaus, 1993c). Principal component analysis uses a loading-score method to compare spectra in multiple dimensions. Sample loadings are obtained by multiplying the spectral data by the principal component scores (proportion of a pattern present in a specific spectrum) which are associated with the largest eigenvalues. Principal components are linear combinations of NIR data that maximize differences between spectra and are calculated by multiplying NIR data points by linear combinations of the spectra to form new variables. The CENTER function ranks each spectrum according to its H distance from the average spectrum in hyperspace.

Principal component analysis is a technique for limiting the number of intercorrelated spectral data points by using the information contained in the spectra to compute independent variables. The first principal component (factor) accounts for the greatest variation in the spectra, the second accounts for the next greatest amount and so on. After ranking the spectra, an algorithm is used to eliminate samples that were spectrally similar. The SELECT algorithm identifies spectra with the greatest number of neighbors within a certain proximity ($H<0.6$) and retains that spectra to represent all of its neighbors, while eliminating the neighbors. Using a standardized H to select samples results in the use of fewer samples than would be recommended by the r^2 method recommended in the USDA handbook (Windham et al., 1989). In experimenting with neighborhood H (NH) limits, Shenk and Westerhaus found that lowering the limit resulted in more samples and more terms being used in the equation. The limit of 0.6 was found to be suitable for defining NH and provided accurate equation predictions. It was unclear as to which factors from neighborhood size, the number of samples, or the number of terms contributes the most to accurate calibrations.

In the next step, the spectra are mathematically treated to emphasize small absorption peaks. Math treatments are typically described by three numbers where the first is the derivative order; second is the segment length over which the derivative was taken; and third, the number of data points in a running average smooth. Both principal components regression and partial least squares regression reduce the data to a few combinations of absorptions which account for most of the information contained in the spectra. However, PLS differs from PCA in that it also relates the sample laboratory reference values to the spectra. Shenk and Westerhaus (1991a) describe "modified"

partial least squares regression method where the lab value data and absorbance data are scaled at each wavelength to have a standard deviation of 1.0 before each PLSR term. Modified partial least squares regression is a full-spectrum regression which uses all regressors to compare factors which correlate with the dependent variable (Fox et al, 1993). Cross validation is conducted by splitting the spectra into equally sized sets according to the file size and using one set to create a calibration equation for predicting the remaining data. Alternately, each set is used to develop an equation for predicting the others until all spectra have been used for predicting and have been predicted. The number of MPLS factors are determined by cross validation so that the standard error of cross validation (SECV) is minimized and the equation is not overfit (Shenk and Westerhaus, 1991a). The number of factors increases until the sum of squared prediction residuals is minimized (Fox et al., 1993). The SECV estimates equation performance using the data from which the cross validation was conducted. Standard error of performance (SEP) is an indication of equation prediction performance with an independent, but similar set of data. Coefficients of determination are computed between each sample spectrum and population average sample spectrum.

The quality and scope of spectra that are used to build a product library determines the accuracy and robustness of a prediction equation developed from spectra in the library. Roberts et al. (1997) found that a prediction equation for ergovaline could only be used for as wide a population as it was developed. Broadening the database from which predictions are developed can broaden the range of prediction, but can result in lower prediction accuracy (Couilliard et al., 1997). To insure adequate prediction equations, a library requires periodic expansion. The algorithms CENTER and SELECT

provide improved population definition for local and global calibration development and techniques have been developed to expand established calibrations. New samples can be analyzed for spectral characteristics that are similar to samples already in the calibration using the MATCH algorithm. By identifying local populations to which new samples belong, local calibrations could be expanded by adding 10 new samples to the library and recalibrating (Shenk and Westerhaus, 1991c).

Applications of Spectroscopy in Site Specific Management

Scientists have been searching for means to efficiently assess the nutrient, stress, and quality status of plants for years. Of special interest has been development of a method for rapid assessment of plant nitrogen content. Traditional methods of N analysis such as the Kjeldahl method for determination of total N or dry combustion analysis involve harvesting tissue, oven-drying for multiple days, and wet laboratory techniques which can be time-, labor-, and materials-consumptive. In the past, instrument assessment of N content in plants has been found to be easier and faster than destructive testing (Ma et. al., 1996). Because N is an important component of the chlorophyll molecule, chlorophyll content is highly correlated with leaf N (Wolfe et al., 1988; Schepers et al., 1992). Procedures have been developed to determine leaf N status by measuring chlorophyll content (Blackmer et al., 1994) and several researchers have found certain wavelengths in the visible portion of the spectrum correlate with chlorophyll content (Gitelson and Merzylak, 1994; Knipling, 1970). Chlorophyll meter readings have been used to estimate leaf N by assessing leaf greenness (Schepers et al., 1992; Wood et al., 1992; Dwyer et al., 1995). Lower concentrations of chlorophyll resulting from nutrient stresses have been detected by assessing leaf reflectance at different wavelengths

(Al-Abbas et al., 1974). Wood et al. (1992) found a high correlation between field chlorophyll measurements at 430 and 750 nm and corn tissue nitrogen . Other research has found that leaf chlorophyll and carotenoid concentrations correlated best with reflectance measured at 550 nm compared to 450 nm and 670 nm (Thomas and Gausman, 1977). Blackmer et al. (1994) used a Minolta SPAD 502 chlorophyll meter to measure transmittance at 650 nm. They chose this wavelength because it lies between two wavelengths associated with chlorophyll activity. Blackmer et al. (1994) and Thomas and Oerther (1972) found that reflectance measurements at 550 nm could be used to detect N deficiencies in corn leaves.

Multispectral radiometry (MSR) is another technique that has been used to assess plant reflectance at different wavelengths. Using a multispectral radiometer to measure canopy reflectance, Ma et al. (1974) found that reflectance measurements correlated to "field greenness". Experiments have been conducted attempting to associate plant physiological stress with chlorophyll. Using a multispectral radiometer, Trenholm et al. (1999) found that single and combinations of wavelengths in the visible and near infrared portions of the spectrum correlated well with visual turf quality, shoot density, and shoot tissue injury ratings. Carter (1994) and Carter and Miller (1994) found the ratio 695:760 nm an indicator of stress due to the "blue shift" phenomenon associated with leaf chlorophyll. In addition, Carter et al. (1996) and Carter and Miller (1994) found that leaf chlorophyll changes due to physiological stress can be detected by MSR instruments. Carter (1993) found wavelengths 535-640 nm and 685-700 nm to be good physiological and herbicide-related stress indicators in forest/shrub canopies.

Identifying instrumentation that can evaluate leaf nitrogen content accurately and

rapidly is paramount to the development of a real-time sensor necessary for integration into a comprehensive site-specific management system. One of the primary goals of sensor-based variable rate technology is to avoid the traditional costs and labor involved in laboratory tissue analysis (Stone et al., 1993). Site specific management of nitrogen can yield monetary and environmental savings for turf managers. Increasing concern for groundwater quality is leading to efficient, economical and accurate assessment of plant nitrogen in many different crops (Blackmer, 1994). This concern for curbing groundwater pollution is echoed by the turf industry. To date, most experiments concerning the practical implications of site specific nutrient applications have dealt with agronomic field crops. Remote sensing of canopy reflectance offers the potential for monitoring plant growth (Bauer, 1975; Walburg et al., 1982) and differential fertilization could be automated by sensing plant-reflected light (Blackmer, 1994).

Various indices have been developed to derive association models between reflectance at specific wavelengths and nitrogen and chlorophyll content and plant biomass (Wanjura and Hatfield, 1987; Thomas and Oerther, 1972). Employing a plant nitrogen spectral index (PNSI) defined as PNSI = ABS [(NIR + red)/(NIR – red)], Stone et al. (1993) used photodiode detectors with interference filters for 671$\pm$ 6 nm (red) and 780 $\pm$6 nm (near infrared) to determine a relationship between spectral radiance and forage yield and forage N uptake to evaluate the potential for correcting in-season wheat N deficiencies. Application of variable fertilizer N based on a PNSI reduced the spatial variation and increased wheat grain yields when compared with application of a fixed N rate. Cassman and Plant (1992) observed an increase in nitrogen use efficiency (NUE) from spatially variable N applications depending on the native nutrient level of the soil.

A normalized difference vegetative index (NDVI) defined as the inverse of PNSI was used by Perry and Lautenschlager (1984) and Duncan et al. (1993). NDVI has been used to correlate ($r^2 = 0.97$) with absorbed photosynthetically active radiation (Asrar et al., 1984) in wheat (*Triticum aestivum* L.) and leaf area index (LAI = NIR wavelength reflectance/Red region reflectance) ($r^2 = 0.96$) in corn (*Zea mays* L.) and soybean [(*Glycine max* (L.) Merr.] (Daughtry et al., 1992). Compared to conventional estimates of plant N, PNSI and NDVI values demonstrated smaller coeffecients of variation (Stone et al. 1993; Ma et al., 1996).

Application of Spectroscopy for Disease Sensing

A number of biotic and abiotic factors, can affect the pattern of the NIR spectra such as plant pigments, leaf blade angle, diseases and plant growth stage (Raikes and Burpee, 1998). In the presence of a disease, a number of physiological changes can occur within the plant (Nilsson, 1995).Indices such as the Leaf Area Index and Normalized Difference Vegetative Index (NDVI) [(NIR reflectance-R reflectance)/(NIR reflectance + R reflectance)] have been correlated with the presence of green biomass and provide a quantitative estimate of general stress on a plant; however, it is often difficult to determine exactly the nature of the stress (Nilsson, 1995). Typically, a given stress reduces photosynthetic capability and causes an increase in reflectance in the red and blue portions of the spectrum and decreased reflectance in the NIR region due to deterioration of leaf tissue (Nilsson, 1995) and leaf structural changes (Raikes and Burpee, 1998). The percent of light reflected in the NIR region provides important information related to the physiological changes in the plant due to disease and provides an earlier indication of stress than visible reflectance (Raikes and Burpee, 1998). Safir et. al. (1991) found that corn infected with southern corn leaf blight (*Helminthosporium*

maydis L.*)* caused higher reflectance in regions of the spectrum related to chlorophyll (0.5-0.7 μm and water (1.45-1.95 μm) regions, indicating that the disease causes other changes to occur.

Several methods have been developed in attempts to quantify the presence of disease symptoms on plants. Infrared aerial photographs have been used with moderate success to remotely sense sugar cane rust fungus (*Puccinia kuehnii*)(Karteris et al.,1980); sugarbeet blackroot disease, one of the causal agents of which is *Rhizoctonia solani* (Schneider and Safir, 1975); and southern corn leaf blight (Safir et al., 1972). Contrary to others, they found that visible reflectance changes preceded infrared reflectance changes. Multispectral radiometry has been used for detection of tomato early blight and rust and late leaf spot of peanut (Nutter, 1987). Multispectral radiometry has been used for detecting dollar spot (*Sclerotinia homeocarpa* Bennett) (Nutter, 1987) and brown patch (*Rhizoctonia solani* Kuhn) (Raikes and Burpee, 1998) on creeping bentgrass (*Agrostis stolonifera* L.) and brown patch and gray leaf spot (*Pyriculara grisea*) on tall fescue (*Festuca arundinacea* L.) (Green et al., 1999). Generally, the purpose of these experiments has been to develop an objective method for assessing disease severity in research plots.

CHAPTER TWO

REMOTE SENSING OF LEAF TISSUE NITROGEN CONTENT IN CREEPING BENTGRASS AND ANNUAL BLUEGRASS USING NEAR INFRARED SPECTROSCOPY

ABSTRACT

Site-specific application of nutrients based upon the specific needs of turfgrass plants has the potential to save money and reduce environmental threats. The objectives of this study were to develop a method to determine N content and of turfgrass in the field and greenhouse using a visible/near-infrared scanning monochromator and evaluate this application for different turf species and different mowing heights. Nitrogen was applied at rates of 0, 1.2, 2.4, 3.6, and 4.8 g N/m^2 periodically over two growing seasons to creeping bentgrass (*Agrostis stolonifera* Huds.) and annual bluegrass (*Poa annua* var. *reptans* Hausskn) mowed at heights of 5 mm and 14 mm. Absorbance was expressed as "log 1/reflectance" between 400 and 2500 nm once color differences were evident. Following spectrometer readings, clippings were harvested from each plot and analyzed for nitrogen using a dry combustion nitrogen analyzer. Modified partial least squares regression analysis demonstrated a relationship (r^2 = 0.78-0.95) between leaf tissue N content and canopy reflectance. Wavelengths which illustrated the greatest differences between lab values for the raw spectrum occurred at wavelengths 670, 1450, and 1930 nm, corresponding to chlorophyll a transmission, a primary overtone O-H stretch attributable to water, and an O-H stretch attributable to water, lignin, protein, nitrogen, and starch. These results indicate the potential for developing a real-time remote sensor for site specific nutrient applications in turfgrass management.

INTRODUCTION

Nitrogen is the mineral nutrient required in the greatest amount for proper functioning of the turfgrass plant. Nitrogen is required for production of amino and nucleic acids, low molecular weight transport molecules, and the proper functioning of chlorophyll (Epstein, 1972). Nitrate and ammonium are the major sources utilized by the plant. Unlike other nutrients, there is no reliable test for soil N. Although rules of thumb are recognized as guidelines, ultimate N application decisions are subjective and based upon a manager's experience with a particular turf (Beard, 1982). Excessive application of N can encourage disease development and reduce tolerance to environmental stress and traffic. Nitrate leaching and subsequent pollution of ground water is an increasing concern, especially on sandy sites.

As golf courses continue to fill the role of urban green areas and are the subject of increased public and governmental scrutiny, a premium is placed upon superintendents to balance environmental impact and playability. Site specific application of nitrogen inputs has the potential to save money, optimize plant nutrition balance and reduce the potential of overapplication and subsequent nutrient leaching. Since N is mobile in the soil and is needed in relatively high amounts (4-5%) by the plant, a sensor capable of attaining a rapid, real-time assessment of turfgrass leaf nitrogen content is necessary for a feasible site specific management program.

Since N is an important component of the chlorophyll molecule (Wolfe et al., 1988; Schepers et al., 1992) procedures have been developed to determine leaf N status by measuring chlorophyll content (Blackmer et al., 1994) and several researchers have found certain wavelengths in the visible portion of the spectrum correlate with

chlorophyll content (Gitelson and Merzylak, 1994; Knipling, 1970). The fact that NIR has been used successfully for constituent analysis of forages lends to its potential effective use in turfgrass analysis (Norris et al., 1976; Windham et al., 1991).

Various indices have been developed to derive association models between reflectance at specific wavelengths and nitrogen and chlorophyll content and plant biomass (Thomas and Oerther, 1972). Employing a plant nitrogen spectral index (PNSI) defined as

PNSI =|[(NIR + red)/(NIR – red)]|, Stone (1993) used photodiode detectors with interference filters for 671 ± 6 nm and 780 ± 6 nm to determine a relationship between spectral radiance and forage yield and forage N uptake to evaluate the potential for correcting in-season wheat N deficiencies. Application of variable fertilizer N based on a PNSI reduced the spatial variation and wheat grain yields when compared with application of a fixed N rate (Stone et al., 1993). Near infrared spectroscopy (NIR) is used for analysis of a wide range of agricultural and industrial products (Wetzel, 1983). Notable agricultural applications have involved measuring protein, moisture, fat, oil, and prediction of organic carbon and total nitrogen (Wetzel, 1983; Dalal and Henry, 1986). Absorbance of NIR radiation corresponds to energy required for changes in the internal vibrational frequencies of the molecule and functional groups of organic molecules absorb NIR radiation differentially. Though not able to measure elemental N directly, NIR has the capability of measuring concentrations of N-H functional groups found in the regions of 1020 nm, 1510 nm, 1980 nm, 2060 nm, and 2180 nm (Hatchell, 1999). The fact that NIR has been used successfully for constituent analysis of forages (Norris, 1976; Windham, 1991) lends to its potential effective use in turfgrass analysis. Fox et al.

(1993) compared reflectance measurements in the NIR region with three other rapid tests for predicting N-supplying capability and grain yield in corn and found that NIRS was as statistically accurate as the pre-sidedress nitrogen test (PSNT) to predict the soil N-supplying capacity and corn response to N.

The objectives of this research were to determine if an association exists between leaf N content and reflectance from the canopy and determine how the relationship is affected by turfgrass species or cultivar, mowing height, and soil type.

MATERIALS AND METHODS

Turfgrass Culture

Field experiments were conducted and repeated during 1998 and 1999 on swards of turfgrass at the Michigan State University Hancock Turfgrass Research Center (HTRC) in East Lansing, MI. The swards consisted of mature monostands of: annual bluegrass (*Poa annua* var. *reptans* Hausskn) grown on an Owosso sandy loam [fine-loamy, mixed, mesic Typic Hapludalfs] and mowed at either 5 mm (*Poa annua* green) or 14 mm (*Poa annua* fairway), Penncross creeping bentgrass (*Agrostis stolonifera* Huds.) grown on a 90:10 (v/v) sand:peat mixture and mowed at either 5 mm (Penncross green) or 14 mm (Penncross fairway), and Providence creeping bentgrass grown on an Owosso sandy loam and mowed at 14 mm (Providence fairway).

Mowing pattern and direction was altered in accordance with typical golf course management practices. To combat any effect of mowing direction on canopy reflectance, mowing was performed in one direction before spectrometer readings were obtained. To avoid possible confounding from the presence of free water on the leaves, dew was removed when necessary. Pesticides were applied as necessary in order to maintain healthy stands of turf during the experiments.

Nitrogen application

Urea ammonium nitrate (UAN; 28-0-0) was applied to each area every 2-4 weeks depending on the growing conditions to produce and maintain turf color and N differences. Treatments consisted of five N application rates of 0, 1.2, 2.4, 3.6, and 4.8 g N/m^2 replicated three times in a randomized complete block design (RCBD). Experimental plots measured 1.2 m x 1.9 m with 0.3-m plot borders. A bicycle sprayer

calibrated for an output of 375 L/ha was used to apply the N solution. Spray applications were made by passing over the plots at 0.7 m/sec with a boom containing three 8002VS nozzles. Following application, plots were irrigated with approximately 40-60 mm water to wash the liquid off the leaves into the soil. Soil acidity, P, and K were adjusted to adequate levels based on soil testing.

Spectrometer Measurements

Spectral reflectance from the turf canopy was acquired with a NIRSystems (Silver Spring, MD) Model 6500 online scanning monochromator. Spectral data were obtained every 2 nm from 400 to 2500 nm and expressed in absorbance units as the log (1/reflectance). The spectrometer was adapted for field use by mounting onto the rear of a garden tractor. The acquired spectral signal was sent to the spectrometer via a fiber-optic cable that was connected to a 30-cm by 15-cm metal box that was mounted onto four 15-cm diameter wheels. The box was suspended approximately 13 cm above the surface of the turf canopy and collected radiation from a 3.5-cm by 12-cm area. The box was designed to minimize the effects of incident solar radiation by shading the area where reflectance measurements were taken. Furthermore, direct light was provided from the box to the measured area using a tungsten-halogen bulb. Three measurements were taken from different locations within each plot during each sampling time. Measurements were taken between the hours of 0730 and 1830 h when visual differences attributable to N were present.

In order to maintain accuracy and repeatability with the instrument, a reference was attained for each scan and the spectrum for the scan was subtracted from that of the reference. In this regard, the NIRS Online 6500 performs similarly to a double beam

spectrometer where a reference and sample spectrum are obtained simultaneously and the differences plotted on the output.

Diagnostic tests were conducted prior to sample readings for repeatability and photometric accuracy. To insure instrument repeatability, diagnostics were conducted prior to sample readings. A Coors ceramic reference plate, which is 80% reflective was scanned once as a reference and again as a sample to measure repeatability. A noise test was conducted by obtaining 32 scans of the reference and 32 more scans using the reference as a sample. The repeatability noise was plotted as the difference between those two sets. The root mean square (RMS) of noise errors across the entire spectra was used to gauge repeatability. Accuracy tests were conducted with a polystyrene standard with known peaks at 1143, 1681, 2166, and 2305 nm (Foss NIRSystems, 1993).

Clipping collection

Following spectrometer readings, clippings were collected with a walking mower. One or two passes were made over each experimental unit with the mower in order to collect enough clippings for N analysis. Clippings were collected from the same swath where scans were obtained. After harvest from each plot, clippings were emptied into paper bags, oven-dried for 72-96 hours at 60° C, ground with a UDY Sample Grinding Mill (UDY Comp., Fort Collins, CO) using a 1mm or 2mm screen, and stored in ethylene oxide-treated plastic bags until N analysis.

Nitrogen Analysis

Clippings were analyzed for percent N by dry combustion method on a Leco CNS-2000 analyzer (Leco Comp., St. Joseph, MI). An amount of 1.00 ± 0.03 g catalyst and 0.1000-0.2300 g of dried and ground sample were weighed into ceramic boats and

homogenized with a microspatula prior to analysis . Apple, tomato, and peach National Institute of Standards and Testing (NIST) standards were alternately queued between 3-4 clipping samples and orchard leaf standards were queued approximately every 10 samples. Each sample was fed into a 1350° C combustion chamber, where all N was converted to N_2 or NO_x. After exiting the furnace, the sample gas flowed through Anhydrone™ (Leco Comp.) tubes and a particle filter before it was collected in the ballast tank. When the ballast was filled, the gas equilibrated before passing through IR cells (for C and S analysis) and an aliquot loop. With He used as the carrier gas, an aliquot doser sends the sample gas to a catalyst heater that reduces all NO_x to N_2. Residual CO_2 and water were removed from the sample by passing through tubes containing $KClO_4$ and Anhydrone™. A thermal conductivity cell consisting of two pairs of matched filaments in a wheatstone bridge configuration detected the amount of N in the sample. The reference pair was in contact with only the He carrier gas; whereas the measurement pair was in contact with the sample gas. Nitrogen contained in the sample gas caused the filament temperature to rise because N has a lower thermal conductivity than He. As the current through the measurement pair changes, the bridge became unbalanced and produced an electrical voltage proportional to the amount of N contained in the sample. The output was then fed to a preamplifier and A/D converter before the digital output signal was used by the computer to display the "percent N" contained in the sample. Following analysis, data was drift corrected by calibration with the orchard leaf. standards (Leco Comp., 1994).

CENTER and Principal Component Development

Spectra were analyzed using the entire spectrum of measurement from 400-2496 nm using ISI chemometric software (Infrasoft International, Port Matilda, PA). Three spectra from each plot were averaged and the average spectrum was matched with the corresponding laboratory N value. A 1,4,4 math treatment was applied to the spectra where the first number is the order of the derivative, the second number is the range in data points (taken every 2 nm) over which the derivative is calculated and the third is the number of data points that are used in a running average smooth (Shenk and Westerhaus, 1991a). Each sample spectrum was ordered according to its distance from the mean spectrum of all measurements taken within a sampling period by the CENTER program (Infrasoft International, Port Matilda, PA). Two passes were made on each file to identify and remove spectral outliers as designated by those spectra with a standardized Mahalanobis (H) distance [Eq.1] > 3.0 or T-value [Eq.2] >2.5.

$$H = (x_I - x_{bar})\,(X'\,X)^{-1}\,(x_I - x_{bar})' \qquad \text{[Eq. 1]}$$

T = (Difference between 2 samples/ standard error of the difference) [Eq. 2]

A principal component analysis file was created on the third pass without removing additional files.

Calibration Equation Development

Software used for all calculations was provided by Infrasoft International, Port Matilda, PA. Using the default setting of the program, ordered files were used for cross validation where one set of samples is used to create a regression equation and the remainder are predicted. All sets are used alternately for equation development until all samples have been used for prediction and have been predicted. Using the best fitted

equation as determined by the cross validation procedure, a coefficient of determination (r^2) was calculated. According to Shenk and Westerhaus (1993c), r^2>0.90 represents acceptable association between spectra values and N values obtained by laboratory NIR instruments during calibration development. Accounting for greater variability in field conditions, r^2 values > 0.80 were deemed acceptable for this study. The calibration method used was a modified partial least squares regression (MPLSR) using detrend, and standard normal variate standardization to create a full spectrum regression model (Shenk and Westerhaus, 1991b; Barnes et al., 1989). Because MPLSR used all 208 wavelengths in the calibration, no calibration equations are shown due to their size and complexity.

During cross validation, each sample spectrum has the opportunity to be predicted as if its laboratory reference value were unknown. The standard deviation of these differences between the predicted value of the sample treated as an unknown and the actual laboratory reference value is the standard error of cross validation (SECV). The SECV values estimate the actual values of the equation when samples are within the global H limits. Using each sample for both calibration and validation of the equation, the lowest model error is used in conjunction with the lowest prediction error to develop an equation with a low performance error. After the equation is created, the difference between the actual N reference values and the predicted N values is calculated. The standard deviation of these differences is the standard error of calibration (SEC). and the SEC describes how well the predicted values fit the regression line.

Standard error of calibration will always be lower than SECV since SEC reflects the fitted values; SECV reflects the actual reference values. The standard error of cross validation is a more accurate means of assessing the equation accuracy than the SEC. The

SECV indicates acceptable equation accuracy if it is lower than the standard deviaiton of the laboratory analysis. The variance ratio (1-VR) is calculated as $1\text{-}SECV^2(SD^2)^{-1}$ where SD = the standard deviation of the laboratory values (Couilliard et. al., 1997). The variance ratio is the ratio of the total variance in the population to the variance predicted by the equation and provides an indication of the accuracy of the model since an accurate model will explain a greater amount of the variation that exists. The coefficient of determination (r^2) calculation involves actual values, while the variance ratio uses predicted values, but in many instances they are similar. Instances where the unexplained variance, determined by the variance ratio, is greater than the SECV would indicate an unacceptable association between spectral analysis and actual N content.

Lab Value Predictions

The MONITOR program was used to predict the laboratory values among species/cultivar, soil type and mowing height by using the equation developed from one population to predict the laboratory N values for another as if they were unknown. For prediction evaluation, the bias was calculated as the difference of the two populations' means and is used as a baseline to adjust the calculated standard error of differences (SED) between spectra. The standard error of differences was expressed as the standard error of performance (SEP) to gauge prediction accuracy in the MONITOR program. The bias confidence limits (0.6 x SEC) were calculated to identify any bias greater than 1.0 x SEC with 90% confidence when using a one tailed Type I error probability = 0.10. SEP(Corrected) limit of 1.3 x equation SEC was used to determine acceptable performance error (Windham et al., 1989).

RESULTS AND DISCUSSION

Laboratory Reference Values

Dry combustion analysis of the turfgrass clippings ranged from 1.47 to 6.28% N for all treatments following N applications ranging from 0 to 4.8 g/m^2 (Table 2.1). A representative VIS-NIRS raw spectra comparison of turf that received a range of applied N is shown in Fig. 2.1. Greatest spectral differences in clipping N content were located at 670 nm, 1450 nm, 1510 nm and 1950 nm and these absorption bands are associated with chlorophyll *a* electron transmissions a primary overtone O-H stretch attributable to water, a first overtone N-H stretch attributable to protein and nitrogen, and O-H stretch and deformation attributable to water, lignin, protein, nitrogen, and starch, respectively (Fig. 2.1). Greatest first derivative spectra differences were observed approximately 30 nm higher than raw spectra differences.

Visible-Near Infrared Reflectance Spectra and Predictions

The first objective of this research was to determine if a relationship exists between the laboratory reference N values and the VIS-NIR spectra. Calculations of H distance by the program CENTER indicate a right-skewed histogram because the median of H values was lower than the mean (Fig. 2.2). Calibration statistics, estimated through cross validation, for the turfgrass swards and their combination are presented in Tables 2.2-2.7. The r^2 (explained variation) and SEC (prediction accuracy) values were 0.92 and 0.25 for the Penncross green, 0.85 and 0.28 for the Penncross fairway, 0.81 and 0.38 for the Providence fairway, 0.80 and 0.45 for the *Poa annua* green, 0.80 and 0.40 for the *Poa annua* fairway, and 0.78 and 0.49 for the combination of all turfgrass swards.

Table 2.1. Laboratory values of nitrogen (N) content in turfgrass clippings.

Treatment	Number of Samples †	Mean N(%)	Range (%)	Std. Dev.
'Penncross' green	83	4.10	2.08-6.28	0.89
'Penncross' fairway	119	3.87	2.15-5.29	0.74
'Providence' fairway	85	4.24	2.37-6.00	0.87
Poa annua green	104	3.38	1.47-5.84	1.00
Poa annua fairway	77	4.07	2.05-6.05	0.91
All treatments	498	3.92	1.47-6.28	0.93

† Number of samples used in development of global equation

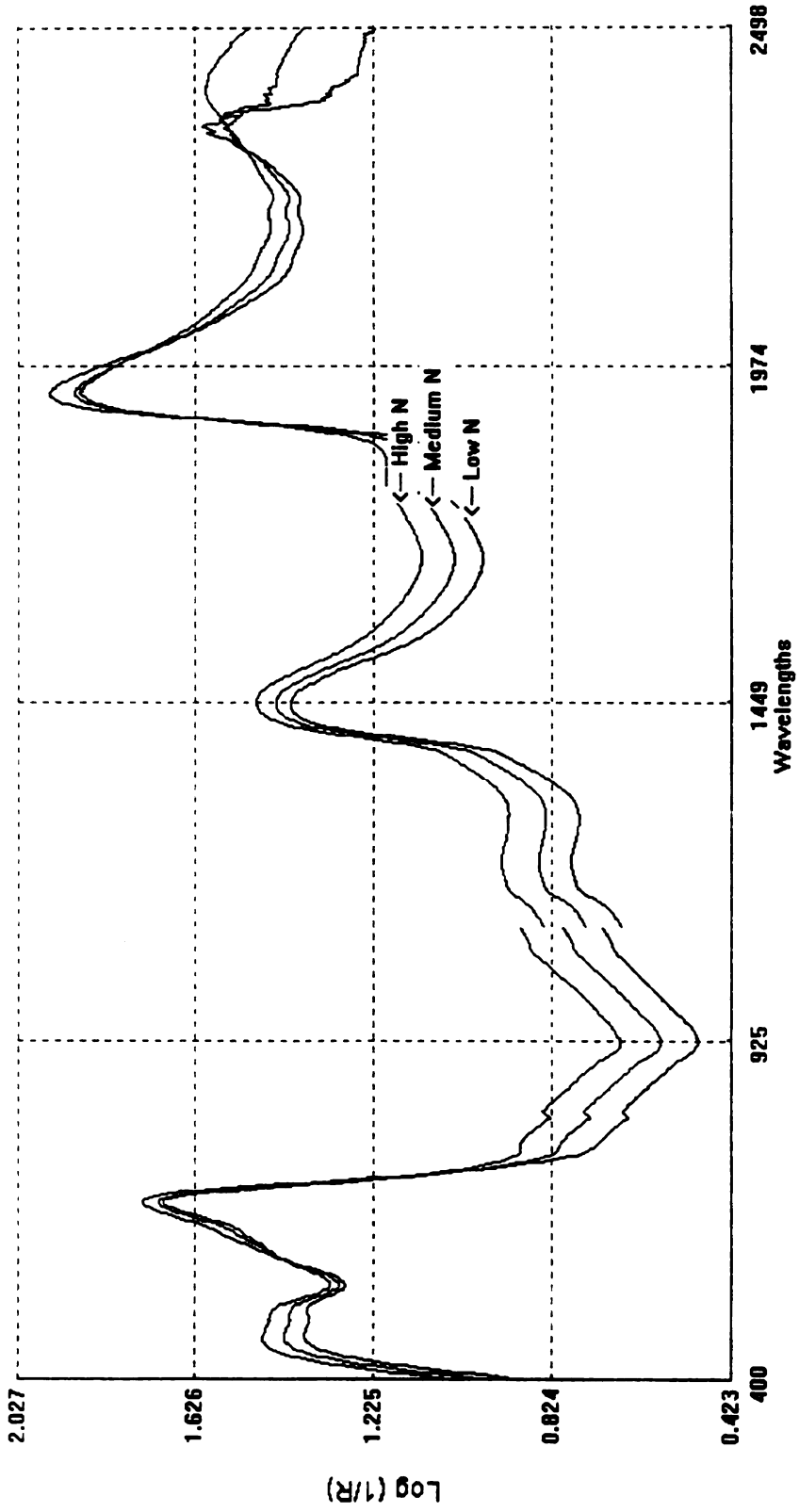

Figure 2.1 Spectra comparison of low range (< 3% N), middle range (3.2-4.0%), and upper range (> 4.5%) average spectra across all measured wavelengths.

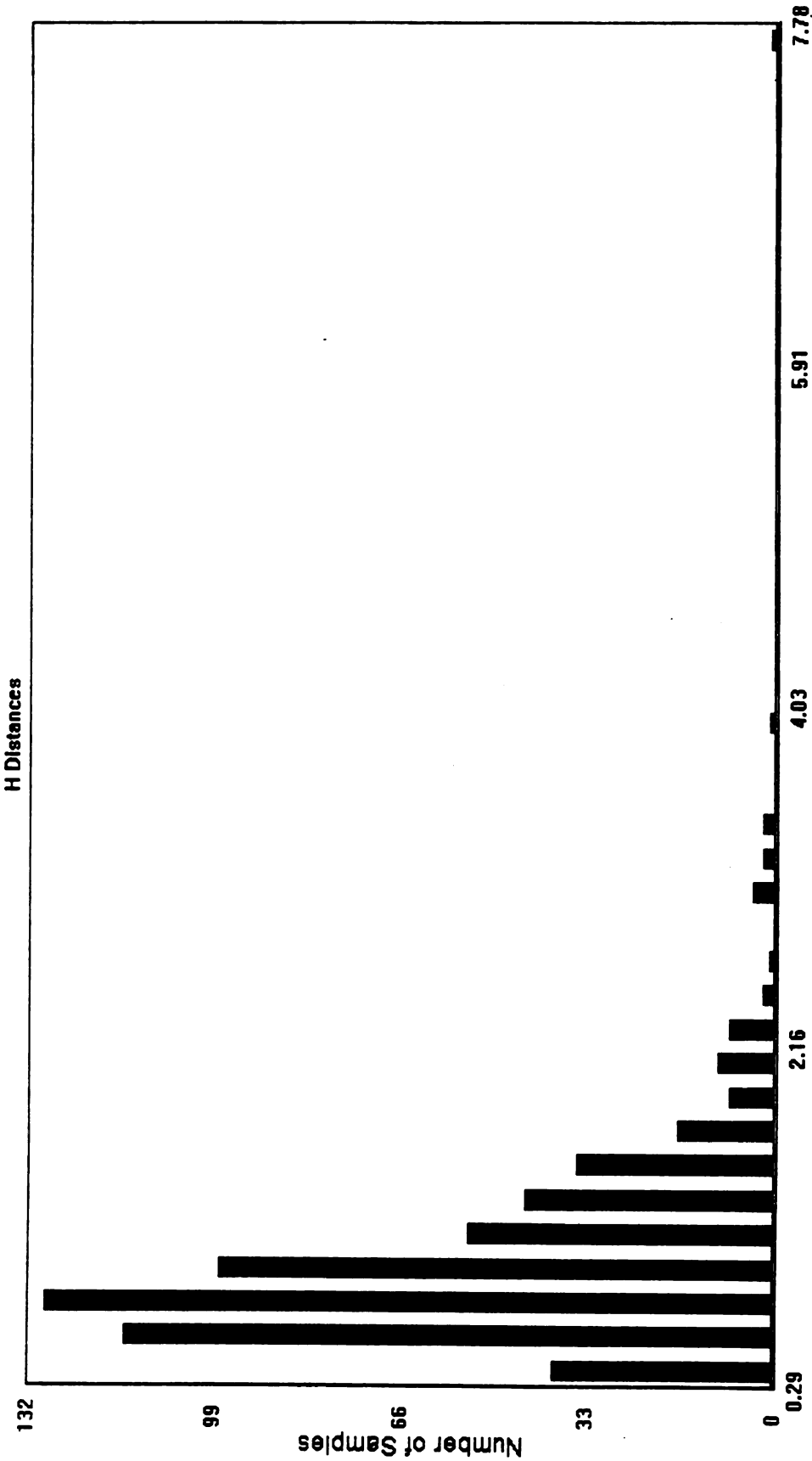

Figure 2.2. Histogram of H distances from the mean spectrum for all samples.

Table 2.2.Calibration statistics for 'Penncross' green combined over both seasons.

Term	Wavelength†	SEC‡	R^2 §	F-value	SECV#	1-VR††
1	686	0.633	0.495	90.29	0.658	0.458
2	1876	0.445	0.75	92.72	0.501	0.686
3	1896	0.405	0.794	19.75	0.464	0.73
4	686	0.359	0.837	24.63	0.525	0.655
5	686	0.302	0.885	37.46	0.744	0.308
6		0.286	0.897	10.59	0.578	0.582
7		0.274	0.905	8.67	0.521	0.66
8		0.267	0.91	5.34	0.43	0.769
9		0.249	0.922	13.55	0.375	0.824

Table 2.3.Calibration statistics for 'Penncross' fairway combined over both seasons.

Term	Wavelength†	SEC‡	R^2 §	F-value	SECV#	1-VR††
1	1896	0.471	0.597	175.87	0.477	0.587
2	1886	0.404	0.704	43.33	0.427	0.669
3	716	0.339	0.792	49.97	0.379	0.739
4	716	0.285	0.852	47.84	0.332	0.800

Table 2.4. Calibration statistics for 'Providence' fairway combined over both seasons

Term	Wavelength†	SEC‡	R^2 §	F-value	SECV#	1-VR††
1	686	0.647	0.447	68.84	0.663	0.425
2	1876	0.571	0.569	24.66	0.598	0.533
3	686	0.536	0.62	11.86	0.558	0.592
4	686	0.429	0.757	46.64	0.481	0.697
5	1886	0.403	0.786	11.80	0.463	0.72
6		0.380	0.809	10.52	0.45	0.736

† Most important wavelength for the first five loading terms used in the equation
‡Standard error of calibration
§ Coeffecient of determination
# Standard error of cross validation
††Explained variance

Table 2.5.Calibration statistics for Poa annua green combined over both seasons.

Term	Wavelength†	SEC‡	R^2 §	F-value	SECV#	1-VR††
1	1396	0.821	0.337	53.27	0.855	0.276
2	1876	0.623	0.618	76.24	0.69	0.529
3	686	0.546	0.706	31.28	0.613	0.628
4	1896	0.49	0.764	25.28	0.566	0.682
5	1396	0.446	0.804	21.49	0.543	0.708

Table 2.6.Calibration statistics for *Poa annua* fairway combined over both seasons.

Term	Wavelength†	SEC‡	R^2 §	F-value	SECV#	1-VR††
1	716	0.692	0.416	55.16	0.764	0.303
2	1876	0.587	0.580	30.21	0.707	0.403
3	1876	0.524	0.666	20.07	0.664	0.474
4	686	0.493	0.703	10.26	0.597	0.574
5	686	0.436	0.769	21.28	0.553	0.634
6		0.403	0.802	13.02	0.53	0.664

Table 2.7.Calibration statistics for all populations combined over both seasons.

Term	Wavelength†	SEC‡	R^2 §	F-value	SECV#	1-VR††
1	686	0.73	0.386	313.86	0.734	0.381
2	686	0.681	0.465	74.25	0.69	0.452
3	686	0.571	0.624	210.44	0.602	0.583
4	1876	0.525	0.682	91.16	0.552	0.649
5	1876	0.475	0.741	111.98	0.515	0.695
6		0.461	0.756	31.36	0.509	0.702
7		0.448	0.769	29.36	0.499	0.714
8		0.435	0.784	29.20	0.491	0.723

† Most important wavelength for the first five loading terms used in the equation

‡Standard error of calibration

§ Coeffecient of determination

Standard error of cross validation

††Explained variance

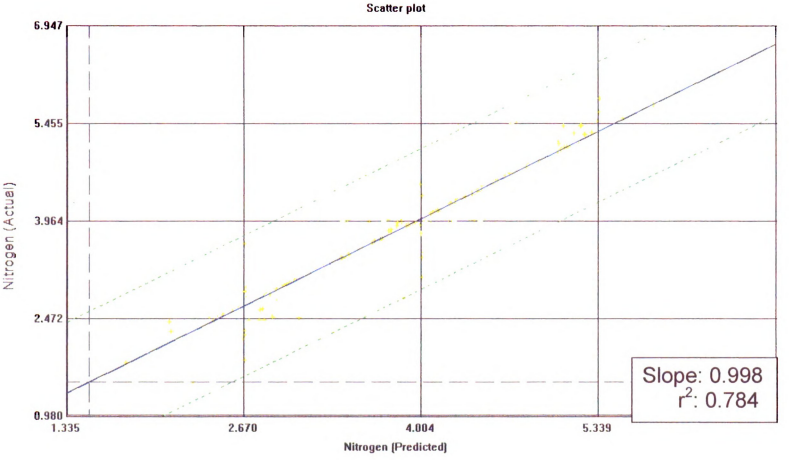

Figure 2.3. Actual *vs.* predicted scatter plot of all samples in global calibration equation. (Solid line indicates slope = 1.00; dashed line indicates actual slope = 0.998; dotted line indicates 95% confidence interval).

Prediction accuracy of the global equation is illustrated graphically in Fig. 2.3. Shenk and Westerhaus (1993c) identified $r^2>0.90$ as acceptable for NIRS applications in the laboratory. Accounting for greater variability under field conditions, $r^2>0.80$ was deemed acceptable in this study. Furthermore, the SEC values for all turfgrass swards were lower than the standard deviation values calculated from the laboratory N analysis (Table 2.1), thus indicating greater prediction accuracy of N using VIS-NIRS compared to conventional laboratory techniques.

The wavelength regions that contributed most to explaining the spectral variation are listed in Tables 2.2-2.7 and shown as both raw and derivatized spectra in Figs. 2.4-2.5. It should be noted that the derivative treatment causes a shift in the spectra. Using derivatized spectra from the 1,4,4,1 math treatment the wavelength regions used most often in equation development were 686-696 and 716-726 nm in the VIS region and 1870-1890, 1386-1396, 1480-1515, and 2360-2380 nm in the NIR region. Figure 2.6 illustrates comparison spectra of the first six eigenvector loading terms used in the creation of the global equation. The wavelengths in the VIS region correspond to green absorbance and have been associated with chlorophyll content in sweet pepper leaves (Thomas and Oerther, 1972), corn (Walburg et al., 1982), and N content in wheat (Stone et al., 1995). The major absorbance peaks for free water and water lattice occur around 1440 and 1900 nm, and 2200 nm, respectively (Bowers and Hanks, 1965; Hunt and Salisbury, 1970). The major absorbance peaks for N-H occur around 1020 nm, 1510 nm, 1980 nm, 2060 nm, and 2180 nm (Hatchell, 1999). Wavelength areas that contributed most to equation development were consistent among turfgrass swards indicating the

Figure 2.4. Raw spectra comparison of the average spectrum of five populations.

1 – Penncross green
2 – Penncross fairway
3 – Providence fairway
4 – *Poa annua* green
5 – *Poa annua* fairway

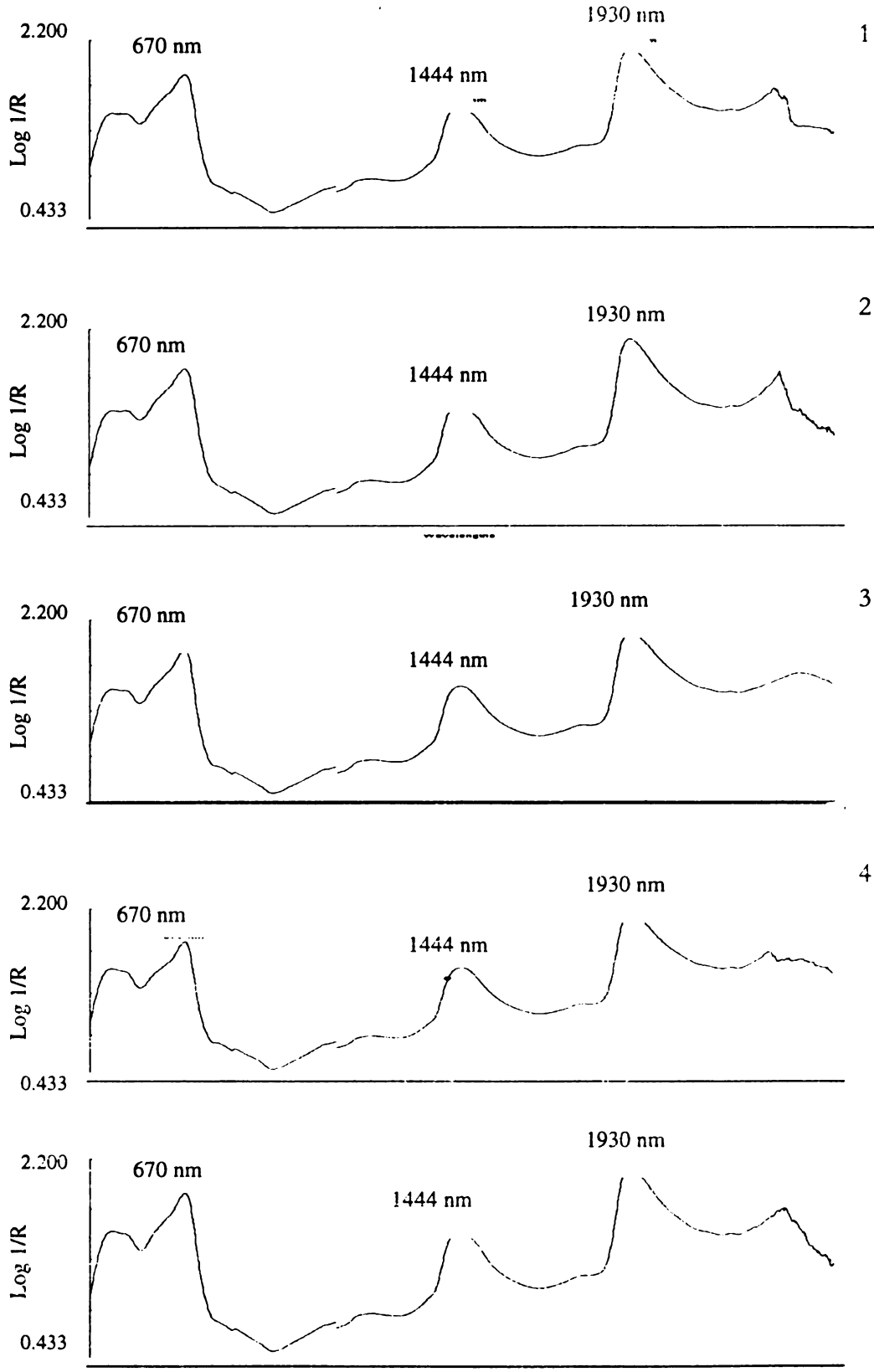
2.200
0.433
Log 1/R
670 nm
1444 nm
1930 nm
1
2
3
4
5

Figure 2.5. First derivative spectra comparison of the average spectrum of five populations.

1- Penncross green
2- Penncross fairway
3- Providence fairway
4- *Poa annua* green
5- *Poa annua* fairway

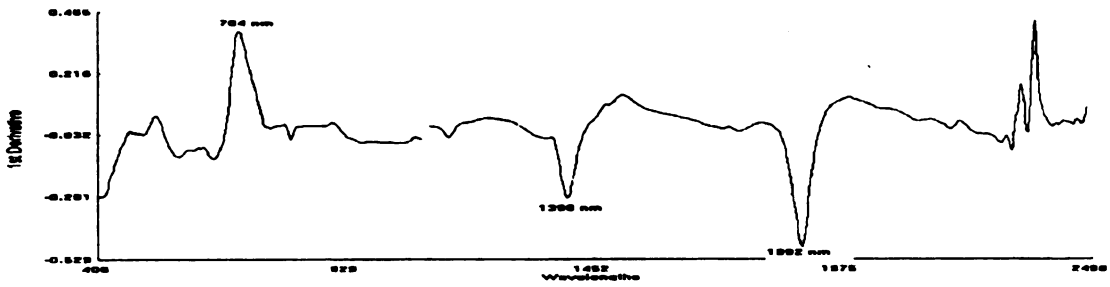
1st Derivative
784 nm
1398 nm
1882 nm
Wavelengths

1


1st Derivative
1398 nm
1882 nm
Wavelengths

2

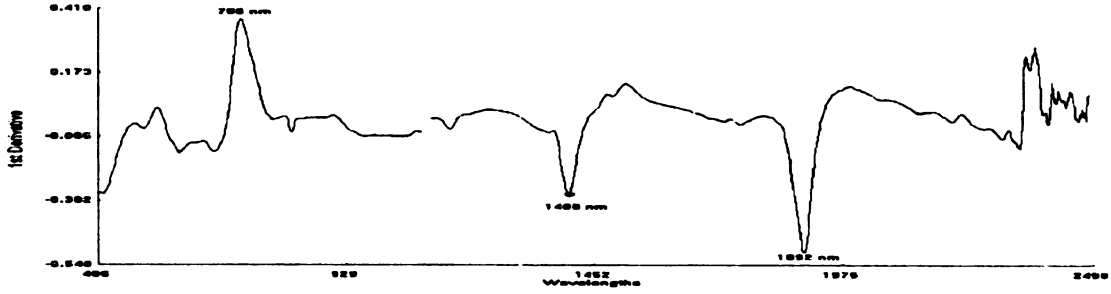
1st Derivative
1400 nm
1882 nm
Wavelengths

3

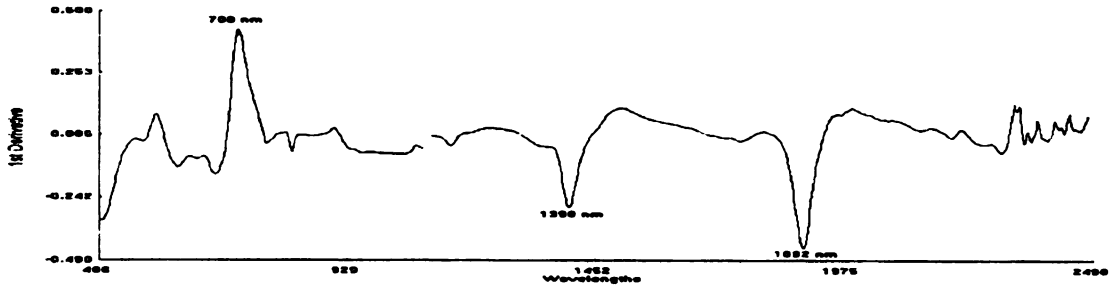
1st Derivative
1398 nm
1882 nm
Wavelengths

4

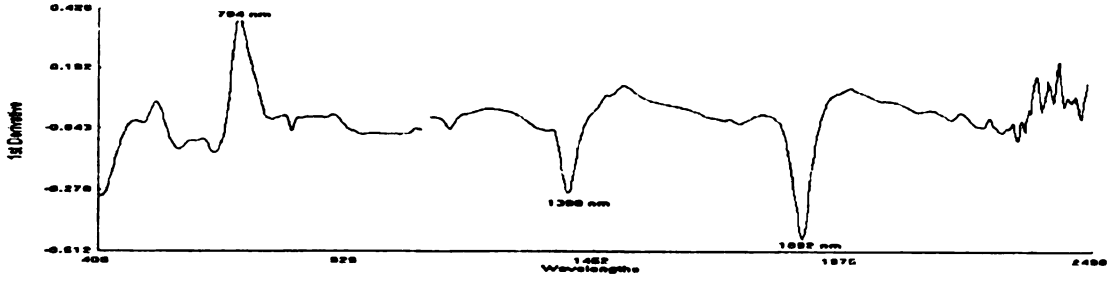
1st Derivative
784 nm
1398 nm
1882 nm
Wavelengths

5

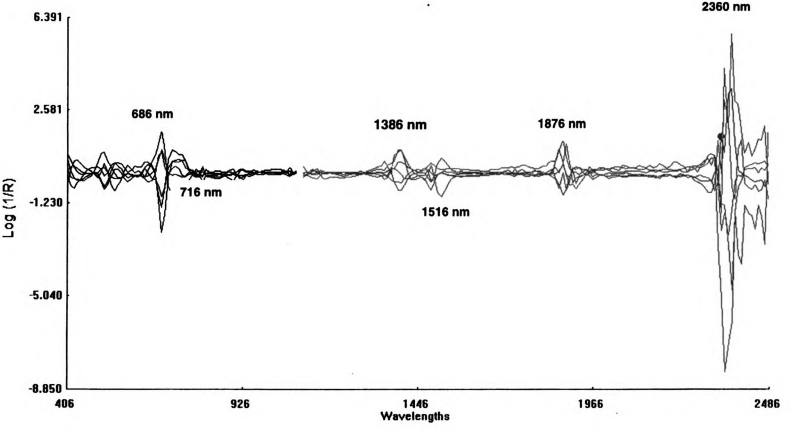

Figure 2.6 Composite graph of loading spectra for the first 6 eigenvector terms used in the global equation.

potential for development of one sensor that could used to predict N in shoot tissue across a range of turfgrass species and cultivars, mowing heights, and soil types (Figs. 2.5-2.6).

Inter-population Predictions

The second objective of this research was to determine how the relationship between VIS-NIRS and N in shoot tissue is affected by species or cultivar, mowing height, and soil type. To accomplish this, N from one turfgrass sward was predicted using the equation developed from another turfgrass sward and vice versa. The comparisons evaluated were: *Poa annua* fairway vs. green on a sandy loam; Penncross creeping bentgrass fairway vs. green on sand:peat; *Poa annua* vs. Providence on sandy loam fairway; and *Poa annua* vs. Penncross creeping bentgrass across soil types. Prediction statistics showing these comparisons are presented in Table 2.8. In general, the ability of one population to predict N from another was very poor and unacceptable for applications in SSM. Coefficients of determination ranged from 0.07 to 0.55 and standard errors of performance (SEP) exceeded the acceptable limited determined as 1.3 times SEC of the equation used for prediction. Poor prediction performance in these experiments indicates that, although there is an association between laboratory N values and spectra patterns, the equations developed in this research were population-specific. These results may due to differences in leaf canopy architecture resulting from different mowing heights, and genetic color differences among species and cultivars. More importantly, however, is the fact that the prediction accuracy inherent in this statistical procedure is optimized by using a broad database of samples. Therefore, it would be difficult to detect an association between two similar but different populations if the

Table 2.8. Statistics for predicting between turfgrass populations for all data combined.

	Population predicted Penncross fairway	Equation predicting Penncross green	Population predicted Penncross green	Equation predicting Penncross fairway
SEP†	0.54		1.60	
Means	3.84	3.72	4.11	3.93
Bias‡	*0.12		*0.18	
Bias Limit	0.11		0.17	
SEP (C)§	*0.53		*1.60	
SEP (C) Limit	0.25		0.37	
Std. Dev.	0.76	0.69	0.89	1.59
Slope	0.81		0.15	
R^2	0.55		*0.07	
Average H#		0.04		73.25*
N	123		92	

	Population predicted Providence fairway	Equation predicting *Poa annua* fairway	Population predicted *Poa annua* fairway	Equation predicting Providence fairway
SEP†	2.29		2.12	
Means	4.28	4.99	*4.12	*4.98
Bias‡	*-0.71		*-0.86	
Bias Limit	0.24		0.23	
SEP (C)§	*2.19		*1.95	
SEP (C) Limit	0.52		0.49	
Std. Dev.	0.91	2.33	0.93	2.01
Slope	0.13		0.14	
R^2	*0.11		*0.09	
Average H#		0.66		0.99
N	96		113	

† Standard error of performance
‡ Mean of differences due to instrument performance
§ Standard error of performance, corrected for bias
# Average Mahalonobis distance from the mean spectrum
*- Outside limit

Table 2.8. Cont. Statistics for predicting between turfgrass populations for all data combined.

	Population predicted *Poa annua* green	Equation predicting *Poa annua* fairway	Population predicted *Poa annua* fairway	Equation predicting *Poa annua* green
SEP†	1.12		1.52	
Means	3.35	3.15	4.11	3.2
Bias‡	0.20		0.91	
Bias Limit	0.24		0.27	
SEP (C)§	*1.11		*1.22	
SEP (C) Limit	0.52		0.58	
Std. Dev.	1.00	1.13	0.97	1.24
Slope	0.41		0.33	
R^2	*0.22		*0.17	
Average H#		0.04		1.06
N	108		94	

	Population predicted All *Poa annua*	Equation predicting All Penncross	Population predicted All Penncross	Equation predicting All *Poa annua*
SEP†	0.89		0.96	
Means	3.71	3.54	3.96	4.12
Bias‡	0.17		-0.17	
Bias Limit	0.17		0.3	
SEP (C)§	*0.88		*0.94	
SEP (C) Limit	0.36		0.64	
Std. Dev.	1.06	0.95	0.83	0.96
Slope	0.69		0.39	
R^2	*0.39		*0.20	
Average H#	not calculated		not calculated	
N	202		215	

† Standard error of performance
‡ Mean of differences due to instrument performance
§ Standard error of performance, corrected for bias
# Average Mahalonobis distance from the mean spectrum
*- Outside limit

prediction equation was based upon only one population. Developing a calibration equation with only one population's data provides a local calibration specific to that species/cultivar and mowing height. To illustrate this point, a separate prediction equation was developed for a portion of the global data set, and then used to predict N from the remaining population. The average r^2 and SEP for the five subsets used in this comparison were 0.65 and 0.58, respectively (Table 2.9). The lower prediction accuracy compared to the overall global equation (Table 2.7) was most likely due to fewer samples used to develop the equation.

CONCLUSIONS

These results indicate that a relationship exists between VIS-NIRS and turfgrass leaf N content. The lower prediction accuracy between laboratory N values and VIS-NIRS spectra demonstrated in this study as compared to other research using the same instrumentation and statistical analysis may attributed to a number of factors. Typical NIRS analysis involves uniform grinding of the sample and use of a laboratory benchtop model for spectral acquisition. Although procedures were taken to minimize the variability due to extraneous factors, conducting experiments in the field and analyzing plants *in situ* lends itself to a veritable plethora of complex influences. Differences in canopy architecture, affected by leaf angle, texture, surface characteristics, mowing height and density, and phenotypic variation among species and cultivars can change reflectance from the plant canopy (Green et al., 1998; Jackson and Pinter, 1986). Since O-H functional group bonding has a considerable affect on spectral absorbance patterns, differences in plant or soil water relations may change the prediction accuracy of N.

Table 2.9. Statistics for predicting subsets of the global equation using the remaind global data for equation calibration.

	Population predicted Subset 1	Equation predicting Global Equation	Population predicted Subset 2	Equation predicting Global Equation
SEP†	0.438		0.674	
Means	3.767	3.785	3.922	4.012
Bias‡	-0.018		-0.090	
Bias Limit	0.440		0.279	
SEP (C)§	0.440		0.672	
SEP (C) Limit	0.678		0.454	
Std. Dev.	0.897	0.790	0.881	0.759
Slope	0.990		0.782	
R^2	0.760		0.604	
Average H#	0.390		0.398	
N	102		102	

	Population predicted Subset 3	Equation predicting Global Equation	Population predicted Subset 4	Equation predicting Global Equation
SEP†	0.594		0.612	
Means	3.975	3.950	3.916	3.870
Bias‡	0.025		0.040	
Bias Limit	0.296		0.280	
SEP (C)§	0.546		0.614	
SEP (C) Limit	0.64		0.607	
Std. Dev.	1.044	0.767	1.028	0.884
Slope	1.123		0.935	
R^2	0.682		0.647	
Average H#	0.393		0.408	
N	104		104	

	Population predicted Subset 5	Equation predicting Global Equation
SEP†	0.603	
Means	3.923	3.952
Bias‡	-0.024	
Bias Limit	0.605	
SEP (C)§	0.605	
SEP (C) Limit	0.676	
Std. Dev.	0.91	0.795
Slope	0.865	
R^2	0.571	
Average H#	0.384	
N	103	

† Standard error of performance
‡ Mean of differences due to instrument performance
§ Standard error of performance, corrected for bias
# Average Mahalonobis distance from the mean spectrum

The practical use of the association between leaf N and VIS-NIRS depends upon the degree of scrutiny desired. The ability to sense and apply N in SSM by explaining 80% of the variation and with 95% accuracy would be an improvement over standard soil testing practices and blanket applications of N. Using SSM, a turf manager would be able to apply N based on an optimal leaf N range between, for example, 4 to 5%. Further research is needed to determine the optimal range of leaf tissue N for various turfgrass species and under different management conditions.

The MPLSR procedure for NIRS has been found to provide greater prediction accuracy compared to other procedures such as stepwise regression (Shenk and Westerhaus, 1991a). According to Couillard et al. (1997) and Shenk and Westerhaus (1993c), the success of using spectroscopy and MPLSR analysis to predict plant and soil constituents is highly dependent upon the development of a broad database of samples with known analysis. Accordingly, this research has only begun to develop such a database to accurately predict N in creeping bentgrass and *Poa annua*. Although MPLSR analysis may be the most useful technique for improving prediction accuracy in NIRS, it is not the preferred technique to analyze how individual factors such as cultivar, mowing height, and soil type affect VIS-NIRS. Therefore, additional analysis is required to determine which wavelengths and wavelength combinations should be used to develop a sensor to detect N or other constituents in different turf environments. Furthermore, this research was conducted under conditions where only one variable was intentionally imposed. To develop an accurate sensor for use in SSM, the influence of other anomalies and their interactions with VIS-NIRS need to be explored. For example, since fungal pathogens affect turf by disrupting phloem translocation and subsequent macromolecule

synthesis and assimilation, an interaction between pathogen presence and N content would be expected.

LITERATURE CITED

Barnes, Dhanoa, Lister.1989. SNV Transformation and De-trending of Near infrared Diffuse Reflectance Spectra, Appl. Spectros. 43:772-777.

Beard, J.B., 1982, Turfgrass Management for Golf Courses, Macmillan Publishing Company, New York.

Blackmer, T.M. , J.S. Schepers, and G.E. Varvel, 1994, Light reflectance compared with other nitrogen stress measurements in corn leaves. Agron. J. 86:934-938.

Bowers, S.A. and R.J. Hanks, 1965, Reflection of radiant energy from soils, Soil Sci. 100:130-138.

Couilliard, A., A.J. Turgeon, J.S. Shenk, and M.O. Westerhaus, 1997, Near Infrared Reflectance Spectroscopy for Analysis of Turf Soil Profiles, Crop Sci. 37:1554-1559.

Dalal, R.C. and R.J. Henry, 1986, Simultaneous Determination of Moisture, Organic Carbon, and Total Nitrogen by Near Infrared Reflectance Spectrophotometry, Soil Sci. Soc. Am. J. 50:120-123.

Epstein, E., 1972, 'Mineral Nutrition of Plants: Principles and Perspectives', Wiley, New York.

Foss NIRSystems, Inc. 1993. Your NIRSystems™ Instrument Performance Test Guide, Foss NIRSystems, Silver Spring, MD.

Fox, R.H., J.S. Shenk, W.P. Piekielek, M.O. Westerhaus, J.D. Toth, and K.E. Macneal, 1993, Comparison of Near-Infrared Spectroscopy and Other Soil Nitrogen Availability Quick Tests for Corn, Agronomy Journal 85:1049-1053.

Gitelson, A., and M.N. Merzylak, 1994. Spectral reflectance changes associated with autumn senescence of *Aesculus hippocastanum* L. leaves. Spectral features and relation to chlorophyll estimation. J. Plant Physiol. 143:286-292.

Hatchell, D.C., 1999, Analytical Spectral Devices technical guide, 3rd ed., Analytical Spectral Devices Inc., Boulder, CO.

Hunt, G.R. and J.W. Salisbury, 1970, Visible and near-infrared spectra of minerals and rocks: I Silicate Materials., Mod. Geol. 1:283-300.

Jackson, R.D. and P.J. Pinter, Jr., 1986, Spectral Response of Architecturally Different Wheat Canopies, Remote Sens. Environ. 20: 43-56.

Knipling, E.B., 1970, Physical and physiological basis for the reflectance of visible and near-infrared radiation from vegetation, Remote Sens. Environ., 1:155-159.

Leco Comp., 1994, Instrumentation For: Characterization of Organic and Inorganic Mehods and Microabsorption Analysis, Leco Company, St. Joseph, MI.

Norris, K.H., R.F. Barnes, J.E. Moore, J.S. Shenk, 1976, Predicting forage quality with NIRS , J. Animal Sci. 43:888-897.

Schepers, J.S., D.D. Francis, M.F. Virgil, and F.E. Below, 1992, Comparison of corn leaf nitrogen concentration and chlorophyll meter readings, Coomun. Soil Sci. Plant Anal. 23:2173-2187.

Shenk, J.S., and M.O. Westerhaus, 1991, Population Definition, Sample Selection, and Calibration Procedures for Near Infrared Reflectance Spectroscopy. Crop Sci. 31:469-474.

Shenk, J.S., and M.O. Westerhaus, 1991, Population Structuring of Near Infrared Spectra and Modified Partial Least Squares Regression. Crop Sci. 31:1548-1555.

Shenk, J.S., and M.O. Westerhaus, 1991, New Standardization and Calibration Procedures for NIRS Analytical Systems, Crop Sci. 31: 1694-1696.

Shenk, J.S., S.L. Fales, M.O. Westerhaus, 1993, Using Near Infrared Reflectance Product Library Files to Improve Prediction Accuracy and Reduce Calibration Costs, Crop Sci. 33:578-581.

Shenk, J.S. and M.O. Westerhaus, 1993, NIR Analysis with Single and Multiproduct Calibrations, Crop Sci. 33:582-584.

Shenk, J.S. and M.O. Westerhaus, 1993, Monograph, Analysis of Agricultural and Food Products by NIRS Reflectance Spectroscopy, PNIS –0120, Infrasoft International, Port Matilda, PA.

Shenk, J.S. and M.O. Westerhaus, 1999, ISI Windows Near-Infrared Software Winisi Monograph version 4.0, Infrasoft International, Port Matilda, PA.

Stone, M.L., J.B. Solie, W.R. Raun, R.W. Whitney, S.L. Taylor, J.D. Ringer, 1993, Use of Spectral Radiance for Correcting In-season Fertilizer Nitrogen Deficiencies in Winter Wheat, Transactions of the American Society of Agricultural Engineers, 39(5):1623-1631.

Thomas J.R., and G.F. Oerther, 1972, Estimating nitrogen content of sweet pepper leaves by reflectance measurements Agron. J. 64:11-13.

Walburg, G., M.E. Bauer, C.S.T. Daughtry, and T.L. Housley, 1982, Effects of nitrogen on the growth, yield, and reflectance characteristics of corn Agron. J. 74:677-683.

Wetzel D.L. 1983, Near-infrared reflectance analysis Anal. Chem. 55:1165A-1176A.

Windham, W.R., D.R. Martens, and F.E. Barton II. 1989, 1. Protocol for NIRS calibration:Sample selection and equation development and validation. p. 96-103. In G.C. Martens et al. (ed.) Near Infrared Reflectance Spectroscopy (NIRS): Analysis of forage quality. USDA Agric. Handb. 643 (revised). U.S. Gov. Print. Office, Washington, DC.

Wolfe, D.W., D.W. Henderson, T.C. Hsiao, and A. Alvino, 1988, Interactive water and nitrogen effects of maize: II. Photosynthetic decline and longevity of individual leaves Agron. Jour. 80:865-870.

CHAPTER THREE

REMOTE SENSING OF DISEASE SEVERITY IN CREEPING BENTGRASS AND ANNUAL BLUEGRASS USING NEAR INFRARED SPECTROSCOPY

ABSTRACT

Brown patch (*Rhizoctonia solani* Kuehn) and dollar spot (*Sclerotinia homeocarpa* Bennett) are two common diseases of cool season turfgrass in the United States. As governmental and public scrutiny of golf course maintenance practices increases, superintendents are beckoned to balance playability with fewer fungicide inputs. The objective of this study was to develop a method of evaluating disease severity using a direct light visible/near-infrared scanning monochromator on creeping bentgrass (*Agrostis stolonifera* Huds.) and annual bluegrass (*Poa annua* var. *reptans* Hausskn). Categorical disease symptom severity ratings of brown patch and dollar spot were made on different turfgrass swards and associated spectra obtained so that absorbance was expressed as "Log 1/reflectance" between 400 and 2500 nm. Discriminant analysis of the data yielded classification accuracy. In the dollar spot study, 20 out of 193 samples (10.3%) were classified incorrectly and in the brown patch study using three severity categories, accuracy improved greatly as there were only 29 misses out of a total of 336 samples (8.6%). These results suggest the feasibility of developing a visible/near-infrared sensor for the detection of disease severity. Future research should address investigation of how various stresses interact to affect the spectral reflectance of the turfgrass plant.

INTRODUCTION

Increasing governmental regulation of pesticides and growing public scrutiny of golf course management practices are leading to the development of improved methods to decrease fungicide inputs on golf courses. As golf courses continue to fill the role of urban green areas and are the subject of increasing public and governmental scrutiny, a premium is placed upon superintendents to balance environmental impact and playability. Although modern chemistry has led to advances on improving fungicide efficacy with lower active ingredient rates, typical management practices involve widespread "blanket" applications of fungicides during periods conducive to disease development. Site specific application of fungicide has the potential to save money, provide an efficient means for effective disease control, and reduce the amount of fungicide applied. Since disease pathogens are dynamic and can infect plants quickly in the presence of optimal growing conditions, a sensor capable of attaining a rapid, real-time assessment of disease status is necessary for incorporation into a site specific management program.

Typically, a given stress reduces photosynthetic capability and causes an increase in reflectance in the red and blue portions of the spectrum and decreased reflectance in the NIR region due to deterioration of leaf tissue (Nilsson, 1995) and leaf structural changes (Raikes and Burpee, 1998). Several methods of remotely sensing plant disease status have been evaluated in past research. Indices such as the Leaf Area Index (LAI) (IR reflectance/Red reflectance) and Normalized Difference Vegetative Index (NDVI) [(IR-R)/(IR+R)] have been correlated with the presence of green biomass and provide a quantitative estimate of general stress on a plant; however, it is often difficult to determine exactly the nature of the stress (Nilsson, 1995). Infrared aerial photographs

have been used with moderate success to remotely sense sugar cane rust fungus (*Puccinia kuehnii*)(Karteris et al.,1980); sugarbeet blackroot disease, one of the causal agents of which is *Rhizoctonia solani* (Schneider and Safir, 1975); and southern corn leaf blight (*Helminthosporium maydis* L.) (Safir et al., 1972). Contrary to others, they found that visible reflectance changes preceded infrared reflectance changes.

The objective of this research was to assess disease severity of two common cool-season turfgrass diseases, brown patch (*Rhizoctonia solani* Kuehn) and dollar spot (*Sclerotinia homeocarpa* Bennett) using a scanning monochromator capable of measuring spectral reflectance from 400-2400 nm.

MATERIALS AND METHODS

Two experiments were conducted at the Michigan State University Hancock Turfgrass Research Center (E. Lansing, MI). The first experiment was conducted to assess dollar spot (*Sclerotinia homeocarpa* Bennett) on swards consisting of mature annual bluegrass (*Poa annua* var. *reptans*, Hausskn) grown on a Owosso sandy loam [fine-loamy, mixed, mesic Typic Hapludalfs], 'Providence' creeping bentgrass (*Agrostis stolonifera*, Huds.) grown on a Owosso sandy loam, and 'Penncross' creeping bentgrass grown on a 90:10 (v/v) sand:peat mix that conformed to United States Golf Association (USGA) specifications. The former two swards were maintained as fairways and mowed at 14 mm and the latter maintained as a green and mowed at 5 mm. Spectrometer readings were obtained from June 16-19, 1999 from portions of the sward naturally infested with dollar spot. Spectra measurements were categorized qualitatively by visual assessment as diseased (diseased); close to the disease but visually healthy (disease front); and visually healthy within the same sward, but not close to disease symptoms. (healthy).

The second set of experiments was conducted to assess brown patch *(Rhizoctonia solani* Kuehn) on a mature sward of 'Penncross' creeping bentgrass grown on a 90:10 USGA sand:peat mix maintained as a green and mowed at a height of 5 mm. Spectrometer readings were conducted during September 2-9, 1999 from areas included in a curative fungicide treatment study. Spectra measurements were qualitatively categorized by visual assessment according to disease severity as severe, moderate, and light.

Spectrometer Measurements

Spectral reflectance from the turf canopy was acquired with a NIRSystems (Silver Spring, MD) Model 6500 online scanning monochromator. Spectral data were obtained every 2 nm from 400 to 2500 nm and expressed in absorbance units as the log (1/reflectance). The spectrometer was adapted for field use by mounting onto the rear of a garden tractor. The acquired spectral signal was sent to the spectrometer via a fiber-optic cable that was connected to a 30-cm by 15-cm metal box that was mounted onto four 15-cm diameter wheels. The box was suspended approximately 13 cm above the surface of the turf canopy and collected radiation from a 3.5-cm by 12-cm area. The box was designed to minimize the effects of incident solar radiation by shading the area where reflectance measurements were taken. Furthermore, direct light was provided from the box to the measured area using a tungsten-halogen bulb. Three measurements were taken from different locations within each plot during each sampling time. Measurements were taken between the hours of 0730 and 1830 h when disease symptoms were present.

In order to maintain accuracy and repeatability with the instrument, a reference was attained for each scan and the spectrum for the scan is subtracted from that of the reference. In this regard, the NIRS Online 6500 performs similarly to a double beam spectrometer where a reference and sample spectra are obtained simultaneously and the differences plotted on the output.

Diagnostic tests were conducted prior to sample readings for repeatability and photometric accuracy. To insure instrument repeatability, diagnostics are conducted prior to sample readings. A Coors ceramic reference plate, which is 80% reflective was

scanned once as a reference and again as a sample to measure repeatability. A noise test was conducted by obtaining 32 scans of the reference and 32 more scans using the reference as a sample. The repeatability noise was plotted as the difference between those two sets. The root mean square (RMS) of noise errors across the entire spectra is used to gauge repeatability. Accuracy tests were conducted with a polystyrene standard with known peaks at 1143, 1681, 2166, and 2305 nm (Foss NIRSystems, 1993).

Data Analysis

Data were analyzed by multivariate discriminant analysis as described by Morrison (1990) using software provided by Infrasoft International (Port Matilda, PA). The three qualitative dollar spot categories were discriminated in the first analysis. In another separate analysis, attempts were made to discriminate among spectra from the three qualitative brown patch disease categories and spectra gathered from a healthy 'Penncross' green during a nitrogen assessment experiment. A third analysis combined all levels of disease (excluding "healthy" samples) for each of the two diseases and attempted to discriminate between the two diseases.

The variables used for classification assume that each population were characterized by a multivariate normal distribution and has a common correlation variate. Following these calculations, cross validation was conducted as described in Chapter 2 so that each set of spectra was used to develop the prediction equation and was placed into one of the categories. Analysis was conducted using the default settings for the DISCRIMINATE program of the Infrasoft Software with a wavelength scanning range from 400-1000 nm and 1100-2100 nm in 4 nm increments and a math treatment of 1,4,4,1 (derivative, gap, smoothing factor 1, smoothing factor 2) without scatter

correction (Shenk and Westerhaus, 1999). Eight cross validation groups were used in creating the prediction equation. In addition to the discrimination comparisons described above, an analysis was conducted to discriminate between brown patch and dollar spot. A 10% error rate for prediction of the samples was deemed acceptable in the evaluation of the results.

RESULTS AND DISCUSSION

Dollar spot study

In the dollar spot study, 20 out of 193 samples (10.3%) were classified incorrectly (Table. 3.1). Comparison spectra for the raw and derivatized data are presented in Fig. 3.1. Attempting to identify the spectra obtained from the "disease front" resulted in the highest percentage of misclassified samples. These results indicate the possibility of identifying the disease before symptoms become manifest; however the question still remains whether this is due only to its close proximity to the disease and if the same results would be measured in a symptom-free sward that is on the verge of developing symptoms. A concern that may contribute to confounding is the fact that the scanning view of the spectrometer was often larger than the diseased area for some scans classified as "diseased." This discrimination suggests the possibility of using information from the VIS-NIR portion of the electromagnetic spectrum for a sensor designed to spray variable rates of fungicide preventatively or curatively for the dollar spot disease.

Brown Patch

Using all four categories, 87 of a total 336 samples (26%) were misclassified (Table. 3.2). Comparison spectra for the raw and derivatized data are presented in Figs. 3.2 and 3.3, respectively. This was most prevalent as "severe" spectra were misidentified as "moderate," and "moderate" spectra mistaken for "light." In an effort to improve prediction accuracy at the expense of reduced prediction precision, the "light" and "moderate" categories were combined and the data were analyzed using three categories for discrimination. Prediction accuracy improved greatly as there were only 29 misses out of a total of 336 samples (8.6%) (Table 3.3). It is unclear whether or not these results

Table 3.1. Predicted v. Actual Category Classification for Dollar Spot Spectra

Spectra Category	Predicted Category: Close	Diseased	Healthy	Total	% of Total	% Error
Close	56	6	6	68	35.2	17.6
Diseased	5	58	1	64	33.1	9.3
Healthy	2	0	59	61	31.6	3.3
Totals	63	64	66	193		
Misses for Category	7	6	7			
Uncertain	22	21	18			

Table 3.2. Predicted v. Actual Category Classification for Brown Patch Spectra Using Four Categories.

		Predicted Category						
		Healthy	Light disease	Moderate disease	Severe disease	Total	% of Total	% Error
Spectra Category	Healthy	68	0	0	0	68	20.2	0.00
	Light disease	0	42	19	1	62	18.5	32.2
	Moderate disease	0	28	73	14	115	34.2	36.5
	Severe disease	1	3	21	67	112	33.3	22.3
	Totals	68	73	113	82	336		
	Misses for Category	1	31	40	15			
	Uncertain	6	41	64	44			

Table 3.3. Predicted v. Actual Category Classification for Brown Patch Spectra Using Three Categories.

		Predicted Category					
		Healthy	Medium disease	Severe disease	Total	% of Total	% Error
Spectra Category	Healthy	68	0	0	68	20.2	0.00
	Medium disease	0	175	17	192	57.1	8.86
	Severe disease	1	11	65	77	22.9	14.3
	Totals	68	186	82	336		
	Misses for Category	1	11	17			
	Uncertain	0	27	16			

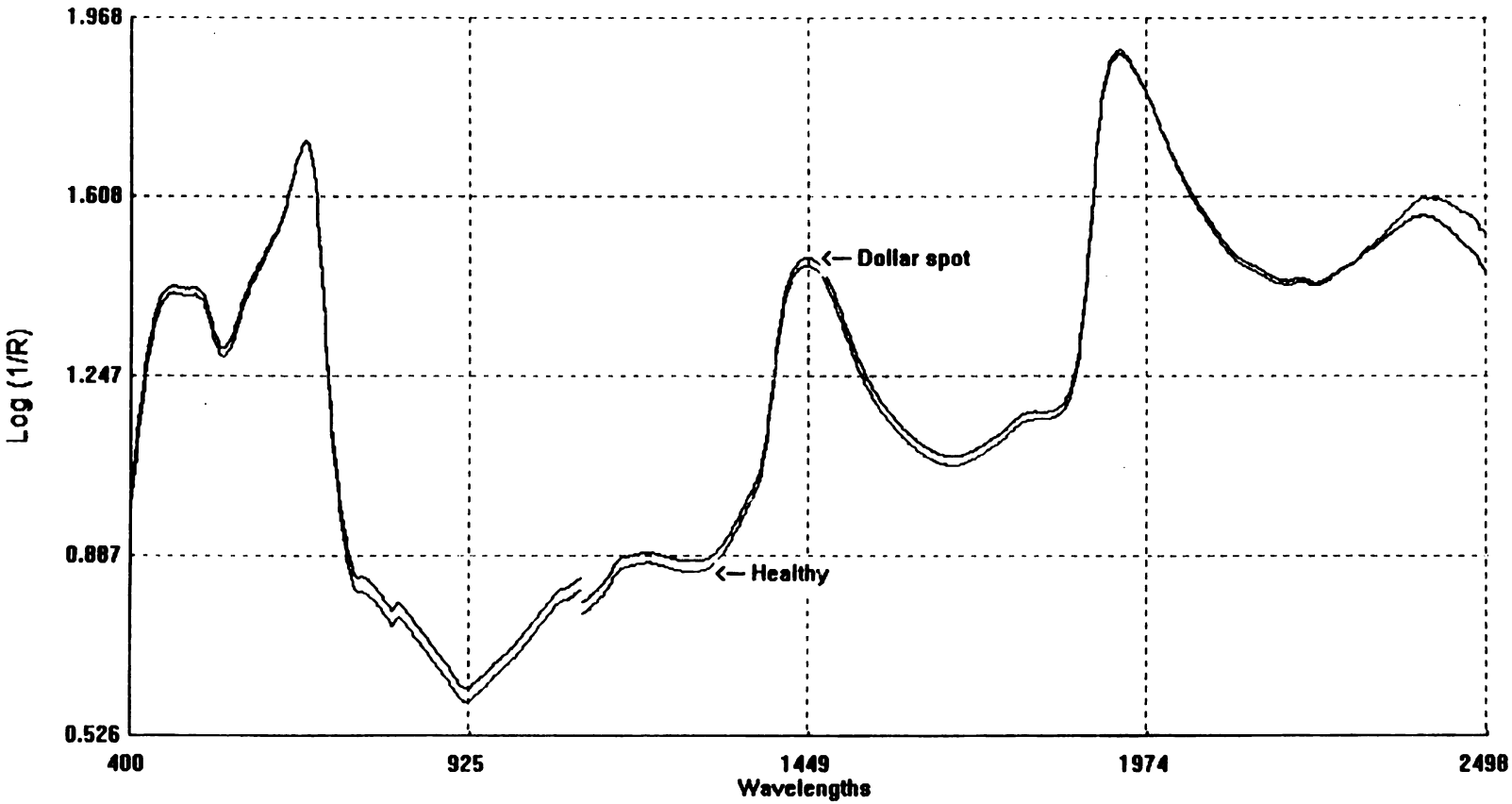

Figure 3.1. Average spectrum comparison of "dollar spot" and "healthy."

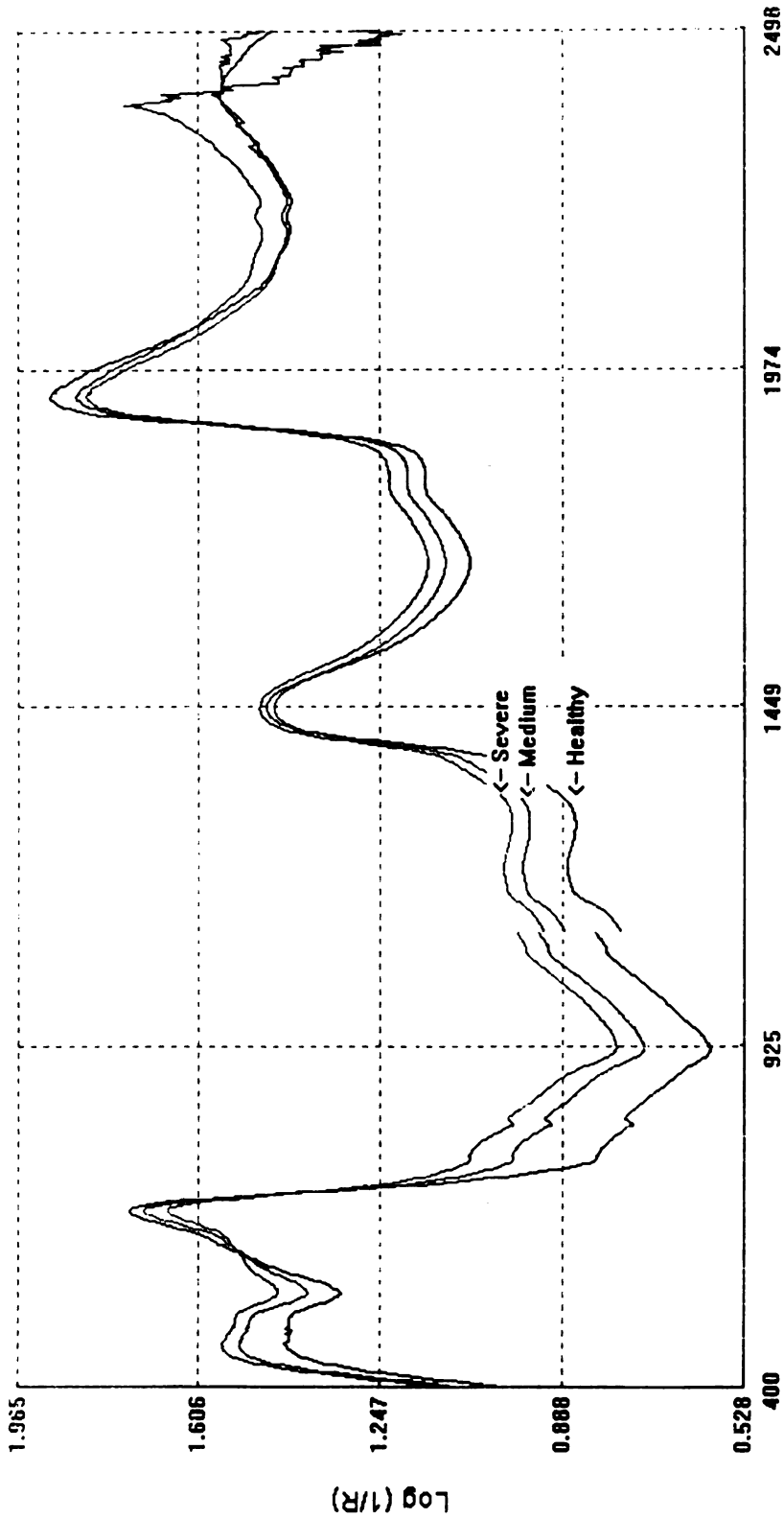

Figure 3.2 Raw spectra comparison for three brown patch disease categories.

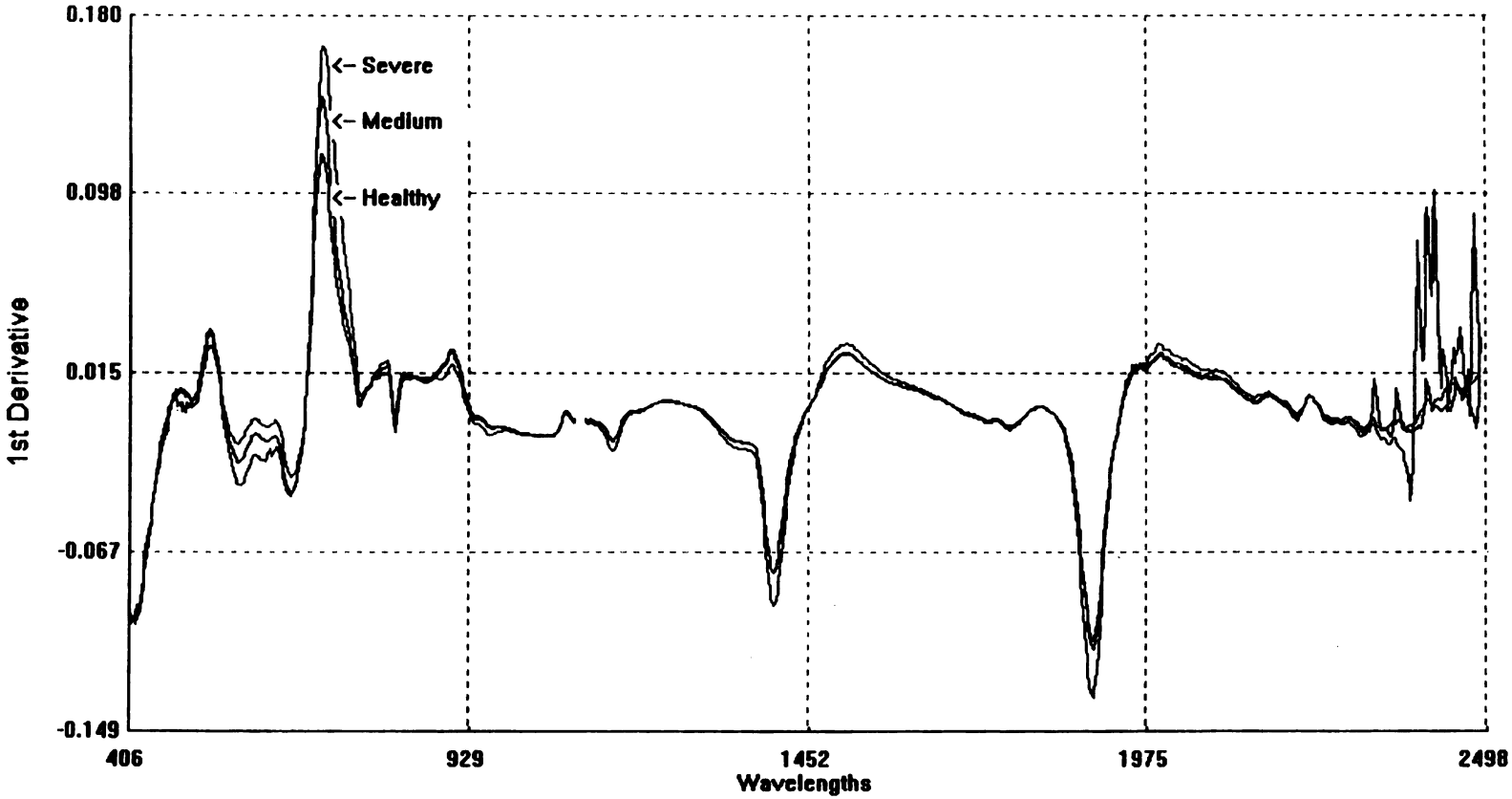

Figure 3.3 First derivative spectra comparison of three categories of brown patch disease.

suggest the subjectivity of qualitative severity ratings and subsequent broad overlap of populations classified as "light" and "moderate". For practical applications, three categories, "healthy", "light-moderate", and "severe" may prove sufficient for effective site-specific applications and subsequent savings in fungicide.

Brown Patch v. Dollar Spot

Combining the three categories of brown patch severity spectra and "diseased" and "front" categories of dollar spot, respectively, analysis was conducted to assess the accuracy of discriminating between the two diseases. Results indicate these populations are significantly different enough to be predicted with 100% accuracy in this particular study; however, the fact that the dollar spot spectra were gathered on 3 different grass swards and the brown patch on only sand-based, green-height creeping bentgrass provides for the strong likelihood of a confounding effect due to grass species, mowing height, and soil type.

CONCLUSIONS

These results indicate that VIS-NIRS is a viable method for assessing brown patch and dollar spot severity. According to the data presented, the spectrometer can qualitatively categorize disease severity with a suitable degree of accuracy. Unlike previous experiments involving the association of turfgrass disease severity with reflectance at discrete spectral wavelengths, the discriminant analysis described above used continuous portions of the visible and near infrared portions of the spectrum for analysis. Previous research indicates that reflectance values measured at 660-, 710-, 760-, and 810-nm and subsequent mathematical combinations of these provide for the best correlation between spectral and disease severity ratings on brown patch and gray leaf

spot (Raikes and Burpee, 1998; Green et al., 1998). The raw data (Fig. 3.2) illustrate spectral differences at these wavelengths and throughout the NIR portion of the spectrum, notably at 1448-nm and 1932-nm. First derivative results (Fig. 3.3) illustrate the greatest differences between categories at 700-, 1400-, and 1930-nm. Because of the various physiological effects produced by pathogens as they degrade leaf tissue, it is difficult to focus on one particular portion of the spectrum for differences in reflectance.

For practical integration into a site-specific management regime, threshold levels of disease need to be developed for proper fungicide treatment. One of the caveats of this technology is the limited amount of data that has been collected. Studies such as these have been conducted by focusing on one anomaly of interest and experimental procedures seek to exclude all other extraneous factors that could affect the absorption pattern of the instrument. However, any interaction effect of multiple anomalies (i.e. water stress, disease, insect damage, chlorosis, etc.) on plant reflectance patterns and their subsequent interpretation is relatively unexplored. To further assess the feasibility of VIS-NIRS technology in site-specific management, experiments need to be conducted exploring interactions among various anomalies.

LITERATURE CITED

Foss NIRSystems, Inc. 1993. Your NIRSystems™ Instrument Performance Test Guide, Foss NIRSystems, Silver Spring, MD.

Green II, D.E., L.L. Burpee, and K.L. Stevenson, 1998, Canopy Reflectance as Measurements of Disease in Tall Fescue. Crop Science 38:1603-1613.

Karteris, M.A., G. Schultink, G.R. Safir, R. Hill-Rowley, 1980, An Evaluation of 70 mm Color Infrared Photography for Sugar Cane Rust Assessment in the Dominican Republic, International Symposium on Remote Sensing of Environment Proceedings.

Morrison, D.F., 1990, Multivariate Statistical Methods, 3rd. ed., McGraw Hill, Toronto.

Nilsson, H.E., 1995, Remote Sensing and Image Analysis in Plant Pathology. Canadian Journal of Plant Pathology 17:154-166.

Raikes, C. and L.L. Burpee, 1998, Use of Multispectral Radiometry for Assessment of Rhizoctonia Blight in Creeping Bentgrass Phytopathology 88:446-449.

Safir, G.R., G.H. Suits, and A.H. Ellingboe, Spectral Reflectance and Transmittance f Corn Leaves Infected with *Helminthosporium maydis*. Phytopathology 62:1210-1213.

Schneider, C.L. and G.R. Safir, 1975, Infrared Aerial Photography Estimation of Yield Potential in Sugarbeets Exposed to Blackroot Disease. Plant Disease Reporter 59:627-631.

Shenk, J.S. and M.O. Westerhaus, 1999, ISI Windows Near-Infrared Software Winisi Monograph version 4.0, Infrasoft International, Port Matilda, PA.

BIBLIOGRAPHY

Al-abbas, A.H., R. Barr, J.D. Hall, F.L. Crane, and M.F. Baumagardener,1974 Spectra of normal and nutrient-defecient maize leaves Agron. J. 66:16:20.

Association of Official Analytical Chemists, Official Mehods of Analysis of Association of Official Analytical Chemists International, Patricia Cunniff, ed., 16th ed., vol. 1, 1997, AOAC International, Gaithersburg, MD, USA ch. 2 pp. 11-13.

Barnes, Dhanoa, Lister.1989. SNV Transformation and De-trending of Near infrared Diffuse Reflectance Spectra, Appl. Spectros. 43:772-777.

Bauer, M.E. 1975, The role of remote sensing in determining the distribution and yield of crops. Adv. Agron. 27: 271-304.

Beard, J.B., 1982, Turfgrass Management for Golf Courses, Macmillan Publishing Company, New York.

Ben-Gera and Norris, 1968, Determination of Moisture Content in Soybeans by Direct Spectrophotometry, Isr. J. Agric. Res. 18:125-132.

Blackmer, T.M. , J.S. Schepers, and G.E. Varvel, 1994, Light reflectance compared with other nitrogen stress measurements in corn leaves. Agron. J. 86:934-938.

Bowers, S.A. and R.J. Hanks, 1965, Reflection of radiant energy from soils, Soil Sci. 100:130-138.

Burpee, L. and B. Martin, 1992, Biology of Rhizoctonia Species Associated with Turfgrasses. Plant Disease 76:112-116.

Carter, G.A, 1993, Responses of leaf spectral reflectance to plant stress, Am. J. Bot. 80:230-243.

Carter, G.A., 1994, Ratios of reflectance in narrow wavebands as indicators of plant stress. Int. J. Rem. Sens. 15:697-703.

Carter, G.A. and R.L. Miller. 1994, Early detection of plant stress by digital imaging within narrow stress-sensitive wavebands, Remote Sens. Environ. 50:295-302.

Carter, G.A., W.G. Cibula, and R.L. Miller, 1996, Narrow-band reflectanceimagery compared with themal imagery for early detection of plant stress, J. Plant Physiol. 128:515-522.

Cassman K.G. and R.E. Plant, 1992, A model to predict crop response to applied fertilizer nutrients in heterogenous fields Fertilizer Res. 31(13): 151-163.

Coleman,S.W., S. Christiansen, J.S. Shenk, 1990, Prediction of Botanical Composition using NIRS Calibrations Developed From Botanically Pure Samples, Crop Sci. 30:202-207.

Couilliard, A., A.J. Turgeon, J.S. Shenk, and M.O. Westerhaus, 1997, Near Infrared Reflectance Spectroscopy for Analysis of Turf Soil Profiles, Crop Sci. 37:1554-1559.

Couch, H.B., 1995, Diseases of Turfgrasses, Krieger Publishing Comp., Malabar, FL.

Couch, H.B. and J.R. Bloom, 1960, Influence of Environment on Diseases of Turfgrasses II, Effect of Nutrition, pH, and Soil Moisture on Sclerotinia Dollar Spot.

Dalal, R.C. and R.J. Henry, 1986, Simultaneous Determination of Moisture, Organic Carbon, and Total Nitrogen by Near Infrared Reflectance Spectrophotometry, Soil Sci. Soc. Am. J. 50:120-123.

Duncan J., D. Stow, J. Franklin and A. Hope, 1993, Assessing the relationship between spectral vegetation indices and shrub cover in the Jornada Basin, NM, Int. J. Remote Sensing 14:3395-3416.

Dwyer, L.M., A.M. Anderson, B.L. Ma, DW Stewart, M. Tollenaar, E. Gregorich, 1995, Quantifying the nonlinearity in chlorophyll meter response to corn leaf nitrogen concentration Can J. Plant Sci. 75:179-182.

Endo, R.M., H.D. Ohr, and E.M. Kraussman, 1964, Phytopathology 54:1175-1176.

Epstein, E., 1972, 'Mineral Nutrition of Plants: Principles and Perspectives', Wiley, New York.

Foss NIRSystems, Inc. 1993. Your NIRSystems" Instrument Performance Test Guide, Foss NIRSystems, Silver Spring, MD.

Fox, R.H., J.S. Shenk, W.P. Piekielek, M.O. Westerhaus, J.D. Toth, and K.E. Macneal, 1993, Comparison of Near-Infrared Spectroscopy and Othe
er Soil Nitrogen Availability Quick Tests for Corn, Agronomy Journal 85:1049-1053.

Gitelson, A., and M.N. Merzylak, 1994. Spectral reflectance changes associated with autumn senescence of Aesculus hippocastanum L. leaves. Spectral features and relation to chlorophyll estimation. J. Plant Physiol. 143:286-292.

Green II, D.E., L.L. Burpee, and K.L. Stevenson, 1998, Canopy Reflectance as Measurements of Disease in Tall Fescue. Crop Science 38:1603-1613.

Hatchell, D.C., 1999, Analytical Spectral Devices technical guide, 3rd ed., Analytical Spectral Devices Inc., Boulder, CO.

Hunt, G.R. and J.W. Salisbury, 1970, Visible and near-infrared spectra of minerals and rocks: I Silicate Materials., Mod. Geol. 1:283-300.

ISI Windows Near-Infrared Software WINISI Monograph, version 4.0, Infrasoft International Inc., Port Matilda, PA.

Jackson, R.D. and P.J. Pinter, Jr., 1986, Spectral Response of Architecturally Different Wheat Canopies, Remote Sens. Environ. 20: 43-56.

Kemp, W., 1991, Organic Spectroscopy, 3rd ed., W.H. Freeman and Company, New York.

Karteris, M.A., G. Schultink, G.R. Safir, R. Hill-Rowley, 1980, An Evaluation of 70 mm Color Infrared Photography for Sugar Cane Rust Assessment in the Dominican Republic, International Symposium on Remote Sensing of Environment Proceedings.

Knipling, E.B., 1970, Physical and physiological basis for the reflectance of visible and near-infrared radiation from vegetation, Remote Sens. Environ., 1:155-159.

Krzanowski, R.M., C.L. Palylyk, and P.H. Crown, 1992, GIS Lexicon In D. Lusch Fundamentals of GIS Workshop, East Lansing, MI.18-19 Aug.1991, Center for Remote Sensing & Geographic Information Science, Michigan State University.

Leco Comp., 1994, Instrumentation For: Characterization of Organic and Inorganic Mehods and Microabsorption Analysis, Leco Company, St. Joseph, MI.

Ma, B.L., M.J. Morrison, and L.M. Dwyer, 1996, Canopy Light Reflectance and Field Greenness to Assess Nitrogen Fertilization and Yield of Maize, Agron. J. 88:915-920.

Marshner, H., 1995, Mineral Nutrition of Higher Plants, 2nd ed., Harcourt Brace and Company, Toronto.

Morra, J.M., M.H. Hall, and L.L. Freeborn, 1991, Carbon and Nitrogen Analysis of Soil Fractions Using Near Infrared Reflectance Spectroscopy, Soil Sci. Soc. Am. J 55:288-291.

Morrison, D.F., 1990, Multivariate Statistical Methods, 3rd. ed., McGraw Hill.

Nilsson, H.E., 1995, Remote Sensing and Image Analysis in Plant Pathology. Canadian Journal of Plant Pathology 17:154-166.

Norris, K.H., R.F. Barnes, J.E. Moore, J.S. Shenk, 1976, Predicting forage quality with NIRS , J. Animal Sci. 43:888-897.

Nutter FW, Jr., 1987, Detection of plant disease gradients using a hand-held, multispectral radiometer (Abstract), Phytopathology 77:643.

Perry, C.R. and L.F. Lautenschlager, 1984, Functional equivalence of spectral vegetation indices. Remote Sensing of Eviron. 14:169-182.

Raikes, C. and L.L. Burpee, 1998, Use of Multispectral Radiometry for Assessment of Rhizoctonia Blight in Creeping Bentgrass Phytopathology 88:446-449.

Roberts, C.A., R.E. Joost, and G.E. Rottinghaus, 1997, Quantification of Ergovaline in Tall Fescue by Near Infrared Reflectance Spectroscopy, Crop Sci. 37:281-284.

Safir, G.R., G.H. Suits, and A.H. Ellingboe, Spectral Reflectance and Transmittance f Corn Leaves Infected with Helminthosporium maydis. Phytopathology 62:1210-1213.

Schepers, J.S., DD. Francis, MF Virgil, and FE Below, 1992, Comparison of corn leaf nitrogen concentration and chlorophyll meter readings, Coomun. Soil Sci. Plant Anal. 23:2173-2187.

Schneider, C.L. and G.R. Safir, 1975, Infrared Aerial Photography Estimation of Yield Potential in Sugarbeets Exposed to Blackroot Disease. Plant Disease Reporter 59:627-631.

Shenk, J.S., and M.O. Westerhaus, 1991, Population Definition, Sample Selection, and Calibration Procedures for Near Infrared Reflectance Spectroscopy. Crop Sci. 31:469-474.

Shenk, J.S., and M.O. Westerhaus, 1991, Population Structuring of Near Infrared Spectra and Modified Partial Least Squares Regression. Crop Sci. 31:1548-1555.

Shenk, J.S., and M.O. Westerhaus, 1991, New Standardization and Calibration Procedures for NIRS Analytical Systems, Crop Sci. 31: 1694-1696.

Shenk, J.S., S.L. Fales, M.O. Westerhaus, 1993, Using Near Infrared Reflectance Product Library Files to Improve Prediction Accuracy and Reduce Calibration Costs, Crop Sci. 33:578-581.

Shenk, J.S. and M.O. Westerhaus, 1993, NIR Analysis with Single and Multiproduct Calibrations, Crop Sci. 33:582-584.

Shenk, J.S. and M.O. Westerhaus, 1993, Monograph, Analysis of Agricultural and Food Products by NIRS Reflectance Spectroscopy, PNIS –0120, Infrasoft International, Port Matilda, PA.

Shenk, J.S. and M.O. Westerhaus, 1999, ISI Windows Near-Infrared Software Winisi Monograph version 4.0, Infrasoft International, Port Matilda, PA.

Shurtleff, 1953, Susceptibility of Lawn Grasses to Brown Patch. (Abstract) Phytopathology 43:110.

Smiley, R.W., ed., 1983. Compendium of Turfgrass Diseases, American Phytopathological Society, St. Paul, MN.

Solomonson, L.P., and M.J. Barber, 1990, Assimilatory Nitrate Reductase: Functional Properties and Regulation, Annual Rev. Plant Physiol. Plant Mol. Biol., 41:225-253.

Stone, M.L., J.B. Solie, W.R. Raun, R.W. Whitney, S.L. Taylor, J.D. Ringer, 1993, Use of Spectral Radiance for Correcting In-season Fertilizer Nitrogen Deficiencies in Winter Wheat, Transactions of the American Society of Agricultural Engineers, 39(5):1623-1631.

Taiz, L. and E. Zeiger, 1991, Plant Physiology, The Benjamin/Cummings Publishing Company, Inc., Redwood City, CA.

Thomas J.R., and G.F. Oerther, 1972, Estimating nitrogen content of sweet pepper leaves by reflectance measurements Agron. J. 64:11-13.

Tisdale, S.L., W.L. Nelson, J.D. Beaton, J.L. Havlin, 1993, Soil Fertility and Fertilizers, 5th ed., Macmillan Publishing Comp., New York.

Turgeon, A.J., 1991, Turfgrass Management, 3rd ed., Prentice-Hall, Englewood Cliffs, NJ.

Trenholm, L.E., R.N. Carrow, R.R. Duncan, 1999, Relationship of Multispectral Radiometry Data to Qualitative Data in Turfgrass Research, Crop Science 39:763-769.

Vargas, J.M., Jr., 1994, Management of Turfgrass Diseases, Lewis Publishers, Boca Raton, FL.

Walburg, G., M.E. Bauer, CST Daughtry, and T.L. Housley, 1982, Effects of nitrogen on the growth, yield, and reflectance characteristics of corn Agron. J. 74:677-683.

Wanjura D.F. and J.L. Hatfield, 1987. Sensitivity of spectral vegetative indices to crop biomass Transactions of the ASAE 30(3):810-816.

Wetzel D.L. 1983, Near-infrared reflectance analysis Anal. Chem. 55:1165A-1176A.

Windham, W.R., D.R. Martens, and F.E. Barton II. 1989, 1. Protocol for NIRS calibration:Sample selection and equation development and validation. p. 96-103. In G.C. Martens et al. (ed.) Near Infrared Reflectance Spectroscopy (NIRS): Analysis of forage quality. USDA Agric. Handb. 643 (revised). U.S. Gov. Print. Office, Washington, DC.

Winisi, 1999, version 1.02a, Infrasoft International Inc., Port Matilda, PA.

Wolfe, D.W., D.W. Henderson, T.C. Hsiao, and A. Alvino, 1988, Interactive water and nitrogen effects of maize: II. Photosynthetic decline and longevity of individual leaves Agron. Jour. 80:865-870.

Woo, K.C., U.I. Fluegge, and H.W. Heldt, 1987, A two-translocator model for the transport of 2-oxoglutarate and glutamate in chloroplasats during ammonia assimilation in the light, Plant Physiology 84:624-632.

Wood., CW, DW Reeves, RR Duffield, K.L. Edmisten, 1992, Field chlorophyll measurements for evaluation of corn nitrogen status. J. Plant Nutr. 15:487-500.

Woolley, J.T., 1971 Reflectance and transmittance of light by leaves. Plant Physiol. 47:656-662.

Zabik, M., 1997, Entomology 893 Course Pack, Mich. State University, E. Lansing, MI.

MICHIGAN STATE UNIV. LIBRARIES
31293020741041